Universidad Zaragoza

1542

Trabajo Fin de Grado

Evaluacion de Diseños de un Convertidor de Turbina de Viento Considerando el Comportamiento Térmico

Evaluation of Wind Turbine Converter Designs Considering the Thermal Behaviour

Autor

Gonzalo Munilla

Director

Rik W. De Doncker

RWTH, Aachen University

2016

Escuela de
Ingeniería y Arquitectura
Universidad Zaragoza

DECLARACIÓN DE AUTORÍA Y ORIGINALIDAD

(Este documento debe acompañar al Trabajo Fin de Grado (TFG)/Trabajo Fin de Máster (TFM) cuando sea depositado para su evaluación).

D./Dª. Gonzalo Munilla Garrido ,

con nº de DNI 73000146D en aplicación de lo dispuesto en el art.

14 (Derechos de autor) del Acuerdo de 11 de septiembre de 2014, del Consejo

de Gobierno, por el que se aprueba el Reglamento de los TFG y TFM de la

Universidad de Zaragoza,

Declaro que el presente Trabajo de Fin de (Grado/Máster)

Grado , (Título del Trabajo)

Evaluation of Wind Turbine Converter Designs Considering the Thermal

Behaviour (Evaluación de Diseños de un Convertidor de Turbina de Viento

Considerando el Comportamiento Térmico)

es de mi autoría y es original, no habiéndose utilizado fuente sin ser citada

debidamente.

Zaragoza, 27/07/2016

Fdo:

Table of Contents

1 Introduction

As a key component in a wind turbine system, the power electronics converter and its power semiconductor devices suffer from adverse power loadings related to environment and other issues, and are proven to have certain failure rates. Therefore, a lifetime estimation of wind power converters is crucial for the improvement of the devices with regard to reliability and also for cost reduction of wind power technology. With the established methods of lifetime estimation and aided by the Rainflow algorithm, information about the reliability performance of wind power converters can be obtained.

1.1 Motivation

The purpose of this Bachelor Thesis is the evaluation of the design of a power electronics converter for wind turbines considering the thermal behavior whilst it is in service. When designing power electronic converters for wind turbines, quite often only the maximum junction temperature is considered. For a wind turbine application, the thermal cycles due to power fluctuations might also shorten the lifetime of power semiconductors. This thermal cycling among different contacting materials with various Coefficients of Thermal Expansion will cause the cracking or deformation in their junctions, thus leading to the failures of the devices. Hence, an overdesign is necessary to increase their life time.

There are, as it will be in detail explained, diverse factors gathered in three different categories which can damage the semiconducorts reducing their life-time. These three categories are named: long-, medium- and short-term thermal loading. This thesis seeks not only to clarify wheather or not the long-term thermal loading of the semiconductors will indeed have a critical impact in their life-time, but also to prove if the medium-term thermal loading effects, which are usually ignored and not taken into account, would indeed have a noticable repercussion as well. We do not take into consideration the loading from the short-term evaluation, as in this thesis we concentrate on the study of the grid side inverter, whose frecuency is of 50 Hz, which is above the values at which the short-term effects play a roll in the life-time as it will be farther explained, aside form the fact that the manufacturers do not present data of their IGBT's, which are tested with frecuencies below this figure, making it impossible at the moment to complete this kind of study.

The use of different designs was also a matter of consideration, so as to observe the different behaviours due to the diverse arrangements and properties when tested in the same conditions. Three types of designs will be tackled: the first two will belong to the same manufacturer, being the third from another. The the first design might be over-rated, which is something we will examine. The reason behind this possible oversizing is to see the existence of significant differences between the other more optimal designs. If these results show indeed noticeable differences, a further study based on their market price and life-span can be carried out to decide whether or not the use of more expensive devices is profitable.

1.2 Structure of the Thesis

The methodology followed along the thesis was as follows:

By means of a simulation model of the power electronics converter and its corresponding thermal model of the semiconductor devices, the thermal behavior of semiconductor devices during the operation can be obtained. This model is connected to two different turbine models: one whose input is the desired generated power; and a second whose input consists on the wind speed and the generated turbulence by the shadow of the turbine. The former will be used for the long-term estimation, being the latter used for the medium-term.

From the connection between each turbine model and thermal model, the junction temperature (T_j) stabilized value and profile can be obtained out of the thermal model for both the long- and medium-term estimation respectively. With these values, we conduct a lifetime estimation by means of the Rainflow algorithm for two different locations where the wind speed along the year holds great differences in intensity. This estimated lifetime is partly calculated by the life-estimation procedure stated by the developers of the IGBT's.

Based on the estimated lifetime of the first design, other two designs will be analysed and compared. Once the results are evaluated, a conclusion and the determination of future work are described.

The simulation models used within this thesis are implemented in MATLAB/Simulink and PLECS.

.

2 Investigated Wind Turbine

The wind turbine under investigation as depicted in Figure 1 is a 2.75 MW wind turbine which is developed at the Center for Wind Power Drives (CWD) RWTH Aachen University for research purposes. The wind turbine has been developed based on the aSiem NM80 wind turbine from the company Vestas. During the development process, the drive-train components are replaced with new ones and the full-converter concept has been selected as the suitable concept for the electrical drive train considering the future development in wind turbine industry.

Table 1 shows the characteristic data of the wind turbine. The nacelle of the wind turbine is situated 80 m above the ground. The rotor blades have a diameter of 80 m that results in a total rotor swept area of 5027 m^2. As it can be seen in the characteristic power curve in Figure 2, the turbine is switched on starting from a wind speed ($v_{wind, cut-in}$) above 4 m/s and reaches its full power at 16 m/s. The power is maintained constant for all wind speeds above 16 m/s before the turbine is shut down once the wind speed ($v_{wind, cut-off}$) exceeds 25 m/s to protect the components from overloads. As can be seen in Table 1, the rotor speed of the low-speed shaft $n_{N, LSS}$ at nominal operation is 15.9 rpm which results in a nominal speed of the high-speed shaft $n_{N,HSS}$ of almost 1100 rpm considering a gearbox ratio r_{gear} of 1:63.
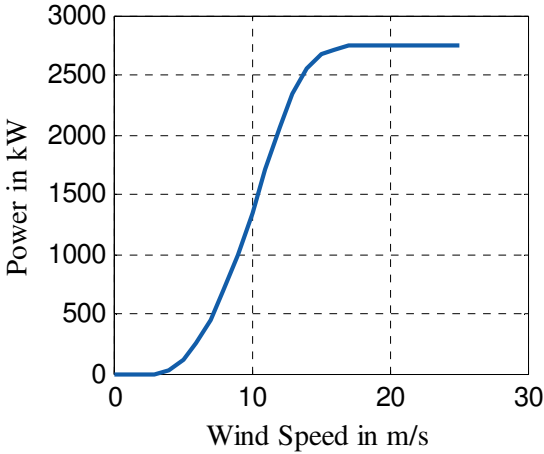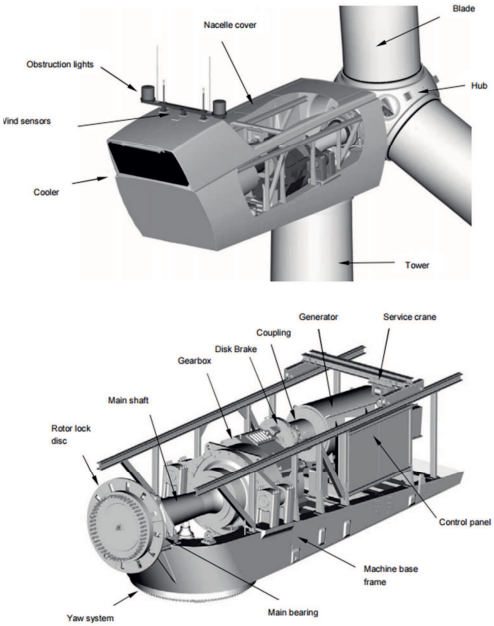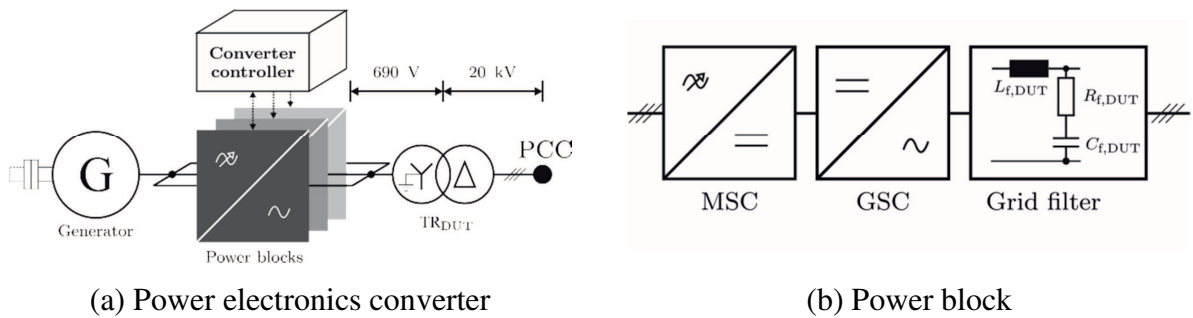

Figure 1 Schematic of the wind turbine NM80 [2]

Figure 2 Power vs wind speed characteristic curve of the wind turbine [2]

Table 1 Parameters of the wind turbine NM80 [2]

Parameter	Symbol	Value
Nominal power	P_{N}	2.75 MW
Rated voltage	U_{N}	690 V
Rotor diameter	D_{rotor}	80 m
Swept area	A_{rotor}	5027 m^2
Maximum rotor speed	$n_{\text{N,LSS}}$	15.9 rpm
Gearbox ratio	r_{gear}	1:63
Control System	-	Pitch-regulated variable Speed
Hub heights	-	80 m

## 2.1 Power-Electronics Converter

In this thesis we study the grid side converter (inverter) shown in Figure 3. This figure represents a three-phase frequency converter, which transforms the ac voltage on the generator side with variable frequency to an ac voltage with a voltage and frequency of 690 V and 50 Hz respectively on the grid side. The converter consists of three similar parallel-connected frequency converters which are synchronously switched by a single controller. This configuration can then be treated as one frequency converter system with a higher rated power. The rated power of the frequency converter has been designed to facilitate the rated power of the generator and a maximum power factor of 0.9. This leads to a converter rated power of 3.05 MVA. With a grid voltage of 690 V, a nominal current of 2552 A on the grid side is obtained, for which the power blocks have to be designed. In table 2 we can observe other parameters of the studied converter.

(a) Power electronics converter   (b) Power block

**Figure 3** The schematic of the considered power-electronics converter for the wind turbine

The power block is constructed by a machine-side converter (MSC) and grid-side converter (GSC) that follows the two-level voltage-source converter as shown in Figure 4. The topology consists of a half-bridge configuration.
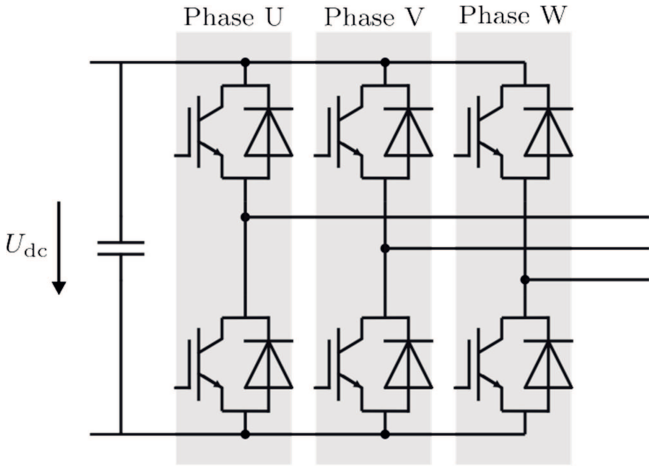
Figure 4 Two-level voltage-source converter (2L-VSC)

The technical advantage of the 2L-VSC solution is the full-power controllability, with relatively simpler structure and fewer components [5]. Figure 5 illustrates the original design of the converter, using another 2L-VSC in parallel in each of the phases. It is this design the one that might be over-rated, as explained in the next page. The use of the first original design would amount in one power block, a total of 24 IGBTs, against the normal optimal configuration, Figure 4, of a total of 12 IGBT's.
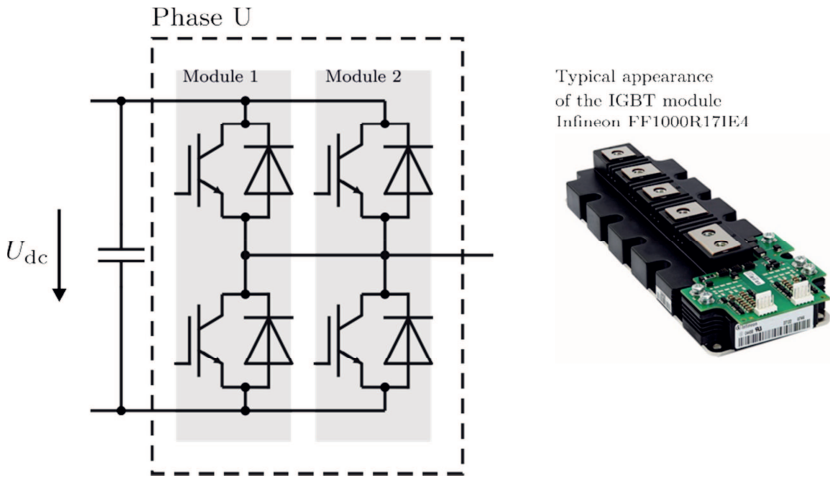
Figure 5 Original design of the phase U of the power block

Table 2 Parameters of the power electronics converter

Parameter	Value
Rated power	3050 kVA
Rated active power	2750 kW
Rated voltage	690 V
Rated current	2552 A
Switching frequency	3300 Hz
Nominal dc-link voltage	1050 V
Modulation strategy	Flat-top modulation

In this thesis, three different configurations of power-semiconductor devices are compared. The detailed data of the considered configuration of power-semiconductor devices is given in Table 3. The design 1 is the original configuration of the semiconductor devices applied in the power-electronics converter of the research wind turbine as explained in Figure 5. It is constructed by the IGBT modules Infineon FF1000R171E4 with a nominal collector current $I_{c,nom}$ of 1000 A. With a total number of IGBT modules of 6 modules per phase, it results in a total peak current capability of 6000 A per phase. Considering the nominal rms current of the converter of only 2552 A as shown in Table 2, it is obvious that the design 1 leads to an overrated configuration for the considered wind turbine.

The second design is constructed using the similar IGBT module as in the first design. However, only the number of modules per phase per power block is reduced to only one module to match with the required nominal current of the converter according to Table 2. The third design has been set with the same target as the design 2. Instead, IGBT modules from ABB with type number HiPAK 5SNA 1600N170100 are used which have a nominal collector current of 1600 A. The design 2 and 3 reflect the typical selection target of semiconductor devices for power-electronics converters regarding the resulting junction temperature at nominal operation ($T_{j,nom}$) which will be explained further in the next subsection.

**Table 3** Electrical characteristics of the considered IGBT modules [7][11] [12]

Parameter		Design 1 (original design)	Design 2	Design 3
Name	Symbol			
Type	-	Infineon Prime Pack FF1000R17IE4		ABB HiPak 5SNA 1600N170100
Blocking voltage	U_{block}	1700 V		1700 V
Nominal collector current	$I_{c,nom}$	1000 A		1600 A
Number of modules / phase / power block	N_{mod}	2	1	1
On-state voltage	u_{ce}	2.35 V		2.6 V
Turn-on energy	E_{on}	390 mJ		530 mJ
Turn-off energy	E_{off}	295 mJ		590 mJ
Reverse-recovery energy	E_{rec}	205 mJ		480 mJ

2.2 Thermal Modeling and Simulation

Thermal model is the key component of this thesis to obtain the estimated behavior of the junction temperature T_j of the power-semiconductor devices during the operation. The junction temperature T_j is required to estimate the lifetime of power-semiconductor devices. The constructed thermal simulation of the power-semiconductor devices which is implemented a simulation model in the software PLECS is illustrated in Figure 6.

Before the two existing kinds of models are explained, two important variables need to be defined: Thermal capacitance and resistance.

• Thermal capacitance is a measurable physical quantity equal to the ratio of the heat added to (or removed from) an object, resulting in a temperature change. Units in Thermal mass.

• Thermal resistance is a heat property and a measurement of a temperature difference by which an object or material resists a heat flow. Units in K/kW.
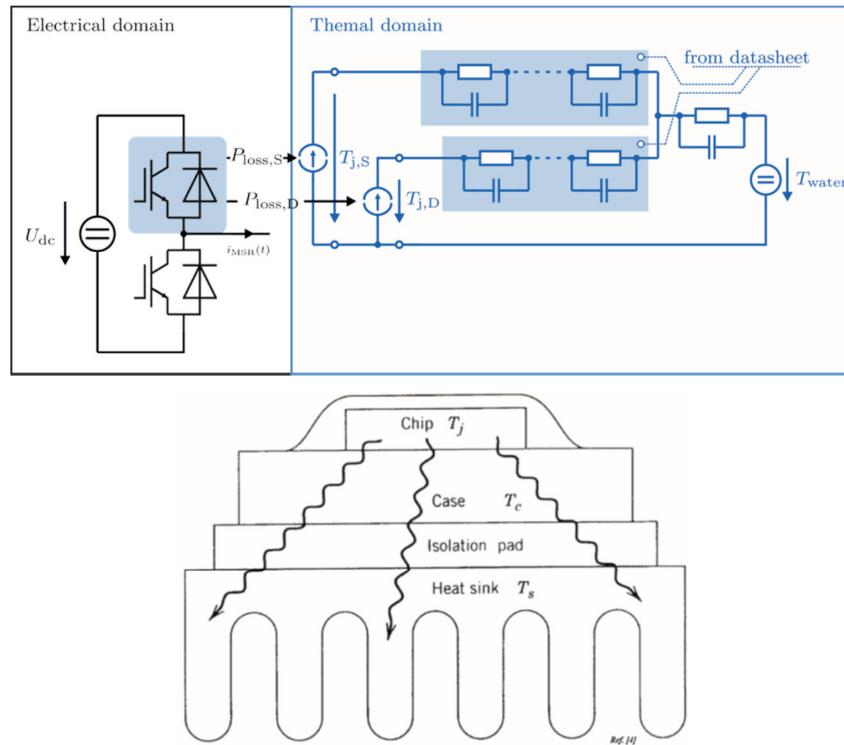
Figure 6 Thermal Foster model and its physical IGBT-Diode modul representation [10]

As we can see in Figure 6, the thermal circuit starts with a "current source", which in a thermal circuits it becomes a temperature source in K, as in the thermal models temperature acts as current on the electrical models. This temperature source represents the junction temperature of the chip, $T_{j,S}$ IGBT, and $T_{j,D}$, Diode, while functioning, which appears due to the heat from the power losses of the devices transfered from the chip to the case, $P_{loss,S}$ IGBT and $P_{loss,D}$ Diode respectively. As both, the IGBT and the Diode, share the same heatsink, both their branches flow into a single parallel thermal resistor and capacitance, which represents the heatsink, in Table 4 can be seen that both share the same value. The ambient temperature that we use in this thesis comes from the one used for the cooling of the devices, which could be appreciated in Figure 6.

There will be a difference between the thermal models of the first design with the second, as the amount of devices in the first design is double. The value of the thermal resistance of the heat-sink for the second and third design is 7.5e-6 in K/kW, therefore, in the other design, the thermal resistance of the heat sink will be greater, exactly double, 1.5e-5 in K/kW; as the heat will need to traverse through two more times material than in the first design.

The thermal behaviour of semiconductor components can be described using two equivalent circuit models:

The first is the Continued Fraction Circuit [3], also known as Cauer model. The continued fraction circuit reflects the physical set-up of a semiconductor: Thermal capacitance with intermediary thermal resistances. The model can be set up where the material characteristics of the individual layers are known, whereby, however, the correct mapping of the thermal spreading on the individual layers is problematic. The individual RC elements can then be assigned to the individual layers of the module (chip, chip solder, substrate, substrate solder, and base plate). The network nodes therefore allow acces to the internal temperatures of the layer sequence.

The other model that can be chosen is the Partial Fraction Circuit [3], represented in Figure 6, in which the RC elements no longer represent the layer sequence. The network nodes do not have any physical significance. This illustration is used in datasheets, as the coefficient can be easily extracted from a measured cooling curve of the module (The representation of time against junction temeperature of the module from the highest temperature reachable until the ambient temperature), and it can also be used to make analytical calculations [3].

The one we chose for our thesis is the Foster model, Partial Fraction Circuit. PLECS does not rely upon the model we use, as any would be transformed into a Cauer circuit, since the inner code of the thermal model is based on that arrangement [9].

By the use of several scripts written in Matlab, the thermal data from the thermal model is extracted and saved into a file which will later be used to calculate the temperature profile over a year for the long-term estimation; and also the 300 s T_j profile of the medium-term estimation will be obtained directly from the thermal model. Table 3 and table 4 provide the cahracteristics of the IGBT's used in this paper.

In Table 4 we can read all the thermal properties of our designs. The heatsink thermal resistance is extracted from this table, but also the ones from the IGBT and Diode will be used in this thesis, introduced in the thermal properties datasheet that PLECS enables for each electronics device. The most relevant aspects of the table are the ones refered to the $T_{j,N}$ of the different designs. It is really interesting to note that there is a 38ºC difference between the 1st and 2nd, supporting the previous estatement about their oversizing, although the end results will determine whether or not this oversizing takes an effect in the lifetime.

Table 4 Thermal characteristics of the considered designs [11] [12]

Parameter		Design 1 (original design)	Design 2	Design 3
Name	Symbol			
Type	-	Infineon Prime Pack FF1000R17IE4		ABB HiPak 5SNA 1600N170100
Thermal resistance heat sink per phase	$R_{th,hs}$	7.5 K/kW		7.5 K/kW
IGBT thermal resistance case to heat sink	$R_{th,c\text{-}hs,sw}$	9 K/kW		12 K/kW
Diode thermal resistance case to heat sink	$R_{th,c\text{-}hs,d}$	18 K/kW		24 K/kW
Temperature of the inlet cooling water	T_{water}	40°C		
Max. junction temperature at nominal power	$T_{j,N}$	81.5°C (IGBT)	119.2°C (IGBT)	120.1°C (IGBT)

3 Thermal Loading Profiles

It is indeed a challenge to map a mission profile of a converter into a loading profile of a power-electronics device. In a wind power system in particular, various dynamical changes of wind speeds or ambient temperatures at time constants ranging from seconds to months, together with the corresponding control behaviors of turbine, generator and converter lead to complicated loading profiles of the devices that are difficult to be handled when doing reliability calculations. The used models in this thesis hereby presented will take into account these dynamical changes and control behaviours, to provide with reliable output data, in order to form consequent reliable temperature profiles, which will likewise be adequate to the length of the timeframes we are studying. Furthermore, a more complete mission profile of power-electronics converter is processed considering different time constants as shown in Figure 7 [4].
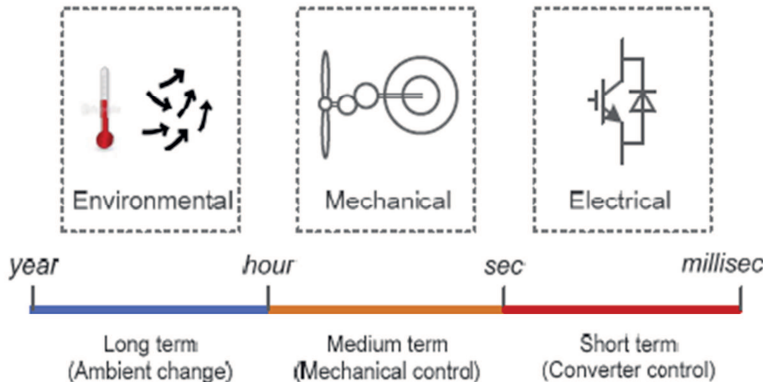
Figure 7 Thermal cycles of power semiconductors with 3 different time constants [4]

These considerations involve multi-physics models with different time constants. It is difficult to evaluate these models together at the same time step in order to acquire the interested thermal behaviors. Hence, the lifetime estimation of the semiconductor devices in power-electronics converter for wind turbines must be separated into three different time frames in which different system phenomenon are considered as shown in Figure 7. In every time frame, different simulation models can be used with different degree of complexity depending of the siginificancy in the corresponding time frame. By doing so, the simulation can be conducted much faster. Finally, the results from every time frame are transformed into an equal scale to be compared.

3.1 Long Term

This group of models and estimations only focus on the long term thermal behaviors and corresponding lifetime caused by the environmental disturbances, for instance, the variation of wind speeds at ambient temperatures in the range of hours. Therefore, simplified models and large time steps are generally used [4]. In our case, it has been considered a one-year wind profile at a constant cooling water temperature of 40º C, as the value of the cooling/ambient temperature barely suffers any changes if the cooling system is propperly designed. Furthermore, the wind data, obtained form two different locations, has been given with a time step of 1 hour.

On the basis of this premise, the flowchart of the lifetime estimation for the long-term thermal cycles of the semiconductor devices shown in Figure 8 is followed. It is impossible to simulate an entire year due to the memory available in the computers used. Therefore, what we seek is mapping, by much shorter simulations, different T_j values for their corresponding torque and operating rotor speed, which is called MPP (Maxium Power Points). Along each of these simulations, torque is constant, generating a constant power, consequently the losses and as a consequence the T_j will stabilize in a small period of time due to the lack of torque variation. That is the reason why we can simulate for 30 seconds, which is the time by which the T_j has estabilized, and not for one entire hour, which corresponds to the wind speed sample time. Therefore, the value of T_j, which we extract from each simulation, will correspond with the last value that our thermal model has registered in this period of 30 s.
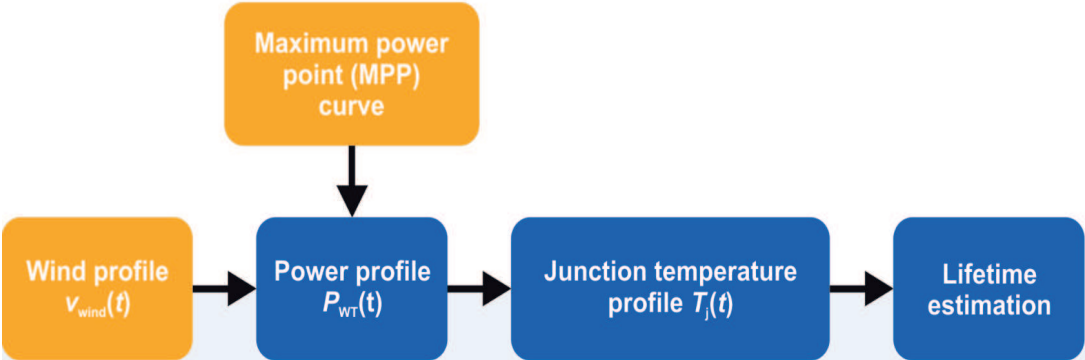
Figure 8 Flow-chart for life-time estimation for long-term thermal cycles

In one hour, the wind, in the way it has been sampled, is constant, which means that the torque produced on the rotor would be constant as well within this hour. This is the basis of the mapping of T_j.

Once we have one T_j for every power, by means of the wind speed profile and maximum-power-point (MPP) characteristic curve we plot the T_j profile for a year, the power profile fed to the electrical grid over the year is obtained. This one year profile is plotted in order to have a year perspective of the lifetime of the divices, which is of more value than having a 3 hour outlook of a turbine that will last several years. Using the junction temperature characteristic of the power semiconductors depending on the converter power, the junction temperature profile over the year can be calculated. Finally, the lifetime estimation can be conducted by means of the rainflow algorithm.

Moreover, the thermal capacitance of materials will lead to fast temperature changes in the power devices ranging among the time constants of seconds to minutes. These temperature changes are however still much smaller than the interested time constants for long term thermal loading. As a result, the thermal capacitance inside the power device as well as the heatsink can be ignored and only thermal resistance is taken into account for long term loading analysis.

3.2 Medium Term

In order to estimate the converter lifetime influenced by the thermal cycles of less than 3 hours, the loading profile with time constants between seconds and minutes has to be established. This group of analysis mainly focuses on the medium term thermal loading of power devices caused by the mechanical behaviors of the wind turbine drive train, for instance the pitch control to limit the generated power and speed control to maximize the power production. Therefore, more complicated models and smaller time steps have to be applied in order to generate enough details of the loading information and thus correctly estimate the lifetime. In this section the analysis is conducted with a time span of 300 seconds in order to restrain the data size. A time step of 15 seconds is applied as the tables given by the manufacturers are scarce and among them this sample time was the one who gave the better scope to identify the most harmful values to the IGBT's.

The wind speed is calculated as an average value over the whole rotor, and it takes the tower shadowing effect and the rotational turbulences into account [2]. Particularly in our system we chose a turbulence intensity of 18%, the worst case scenario [2]. It seems as if the process for medium term estimation is straight forward, but it holds some differences against the long-term estimation, as we will see on the following pages, though its essence can be simplified into Figure 9.
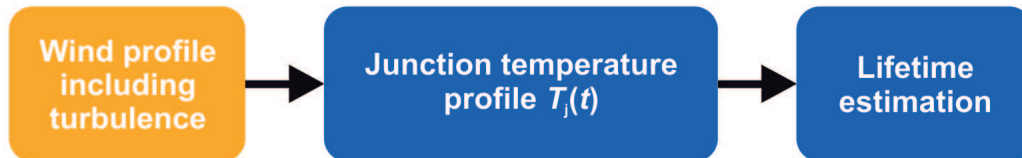
Figure 9 Flow-chart for life-time estimation for medium-term thermal cycles

Contrary to the previous estimation, the T_j will not stabilize in 300 seconds of simulation. The T_j values we would obtain are random through this period of time due to the variability introduced by the turbulence. But at the same time, accordant to the values of the input, which in this case is directly the wind speed and the fixed turbulence.

Afterwards, we extrapolate this 300 seconds profile to 3 hours and apply the procedure of the lifetime estimation.The choice of this intervals will be later explained. All this process will be repeated for each particular average wind speed ranging from 4 m/s to 16 m/s, the reason of the use of this interval is explained in point 4.2. Once we have the lifetime value for each wind speed, we multiply these values by the weights of the wind speeds (percentage of time that particular wind speed has taken place along the year), and then we add them together. We follow the procedure of the Miner's Rule.

In contrast to the long-term lifetime analysis, the thermal capacitances of the materials constructing the IGBT modules play a siginificant role in the resulting thermal cycles of the junction temperatures. This is because the thermal time constant of the materials is in the range of seconds to minutes. Hence, the thermal dynamics are no longer negligible since it is in the range of the investigated time frame.

3.3 Short Term

In order to estimate the converter lifetime influenced by the short-term thermal cycles of less than 1 second, a loading profile with time constants of milliseconds has to be established. This group of thermal behavior is mainly caused by the fast electrical disturbances of the converter

such as load current alternating, or the impacts of grid faults, switchings, etc. Therefore, small time steps are generally required for this analysis. This group of thermal loading in power devices is mainly caused by the fast and periodical current alternating in the converter, the junction temperature of power devices swings at a relative smaller amplitude and at a constant frequency, in this case the grid's, which is of 50 Hz. At this frequency, though it seems low, it is high enough (The time periods are small enough), so as not to play an important roll in the inverter. But, if we happen to study the rectifier, on the machine side, the fundamental frecuencies shall be much lower than 50 Hz, and therefore, this time periods would be important enough to take them on account. In addition to the fact that we are studying solely the inverter, the proper information from the manufacturers to test possible results at lower fundamental frecuencies than 50 Hz is not available, therefore no testing can be done on our behalf.

The temperature increase obtained in this term would be periodical and would follow the fundamental frecuency of the system. As long as an increase of intensity occurs, the temperature will do so as well. When the IGBT does not conduct in the second half of the period, the IGBT will cool down. This heating and cooling cycle is the stress exerted on the IGBT that the one the short-term analysis considers. For 50 Hz of fundamental frequency, a 20 ms cycle time would be considered, but even though it will not play an effect in the inverter, the over-all procedure is hereby explained:

With the information of temperature mean value T_{jm} and cycling amplitude ΔT_j the lifetime models can be directly applied without rainflow counting as shown in (1) and (1) [4].

$$\Delta T_j = P_{loss}.Z_{th}.\left(\frac{3}{8f_o}\right) + 2.P_{loss}.Z_{th}.\left(\frac{1}{4f_o}\right) \tag{1}$$

Values obtained from the manufacturer's datasheet for ΔT_j:

- Power losses in the device: $P_{loss} = f\ (P_{converter}, T_j)$
- Time-based thermal resistance: Z_{th}
- Fundamental frecuency of the converter output = cycling frequency of the interested thermal loadings: $f_o = 50$ Hz

$$N_{life} = 1.017^{\left(125-T_{jm}-\frac{\Delta T_j}{2}\right)^{1.16}} \times\ 8{,}2.\,10^{14}\ (\Delta T_j)^{-5.28} \tag{1}$$

15

It is also noted that because of the relative larger thermal capacitance in the case, the thermal dynamics of the case temperature is not as fast as the junction temperature; thereby the case temperature is not considered for the life time estimation by short term thermal loadings. This process also does not seem complicated, though it holds the same intricacy when it comes to calculate the N_{life} as it occurs with the medium-term method. But as we do not take this lifetime estimation into account, for the high frequency at which we are working, we will not get into details.

4 Thermal Behavior of Semiconductor Devices

4.1 Long Term

The first model which we used to calculate the thermal data in order to obtain the temperature profile has been developed in another project and available at the Institute PGS. Through its connection to the thermal model of the converter we created, we obtained the results for the various T_j vs. the power for each design which can be seen in Figure 10, Figure 11 and Figure 12. We can see that none of the graphs starts under 40 ºC (This water cooling temperature, is also named in this paper ambiente temperature, T_A) due to the temperature of the constant inlet of cooling water, therefore, it is the maxium Tj allowed before the designs are overheated. Also there is clearly an increment in T_j as power rises. This is due to the efficiency of the devices, with more power generated, the more power losses which become heat will be produced, rising the T_j at the same time.
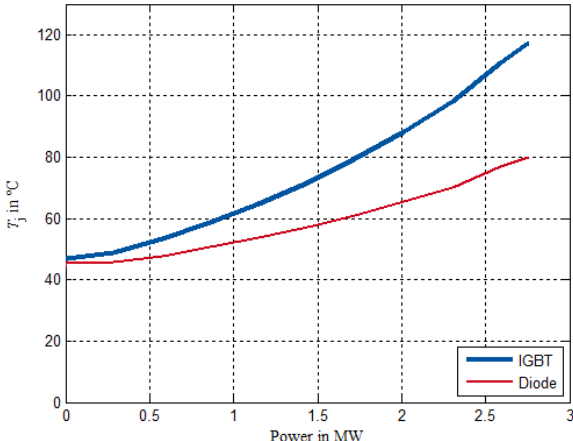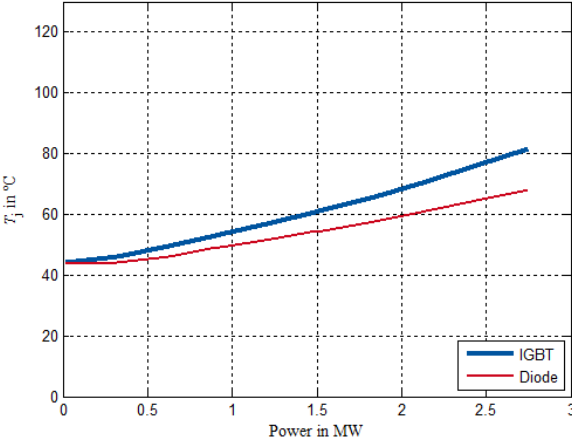
Figure 10 Characteristic line of the design 1   **Figure 11** Characteristic line of the design 2
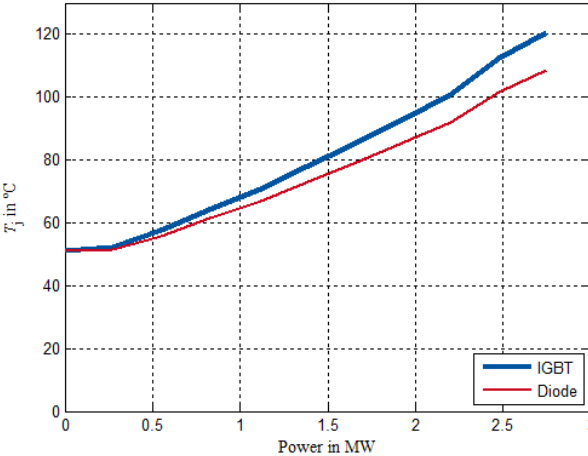
Figure 12 Characteristic line of the design 3

Table 5 IGBT temperatures at the nominal power of 2.75 MW

Temperatures at the nominal power of 2.75 MW	T_{j_max} with T_{water} 40ºC
Design 1	81.5 ºC
Design 2	122.1 ºC
Design 3	120.1 ºC

First conclusions analyzing our first set of data from Table 5:

- The hottest device is the IGBT instead of the Diode since the grid-side converter (GSC) is operating in the inverter mode during the normal operation. In the inverter mode operation, the IGBT conducts more compared to the Diode resulting in higher dissipated losses. Hence, the junction temperature of the IGBT is greater than the diode.

- The 1st design has a lower increment of temperature than the rest. This is due to the fact that it is conducting much less amount of current as the other two designs, half. Though this brings the question about why designs 2 and 3 share more or less the same high temeperature if they are able to conduct different nominal collector current. The answer to this can be seen in the thermal resistance of Table 4, the ones from the design 3 are higher than the ones from designs 1 and 2. Consequently, even though design 3 is capable to withstand more current, their losses will be greater due to a higher resistance against the heat flow, hence the similarity of the results. It can be observe that the Diode resistance of design 3 to heat flow is 6 units larger than in the other two designs, difference that can also be seen in the Diode curve of design 2 and 3.

- The junction temperature of the design 1 is far below the maximum allowed junction temperature (150° C). This is an indication that the first design has more power capability than required for the considered wind turbine. The other two designs are right below the optimal temperature of functioning of 125ºC, temperature the developers use always as normal conditions of functioning [11].

- We can prove now with solid data that the first design is over-rated for the long-term estimation as it does not reach optimal temperatures of use.

Once the arrays of coupled values of T_j and power are obtained, they are later used to create the junction temperature profiles of the IGBT and diode for one year.

For that, a 1-year wind profile and Figure 2 were needed in order for Matlab to calculate the 1-year power profile. Being not content with only one location, the used data corresponds to two different locations: Feldberg and Leuchtturm Alte Weser in Niedersachsen. This data was retrieved in 2013 by their correspondent wheather stations in the area. Compared to the second location, the first location (Feldberg) shows relatively lower wind intensity. It can be seen that the wind turbine barely reaches at some points the nominal power of 2.75 MW. On the other hand, the second location holds stronger wind intensity, exerting enough torque in the turbine rotor, thus reaching in many time-spans the nominal power as can be seen in Figure 16.

Figure 13 and Figure 15 show the gathered wind profiles over a year.
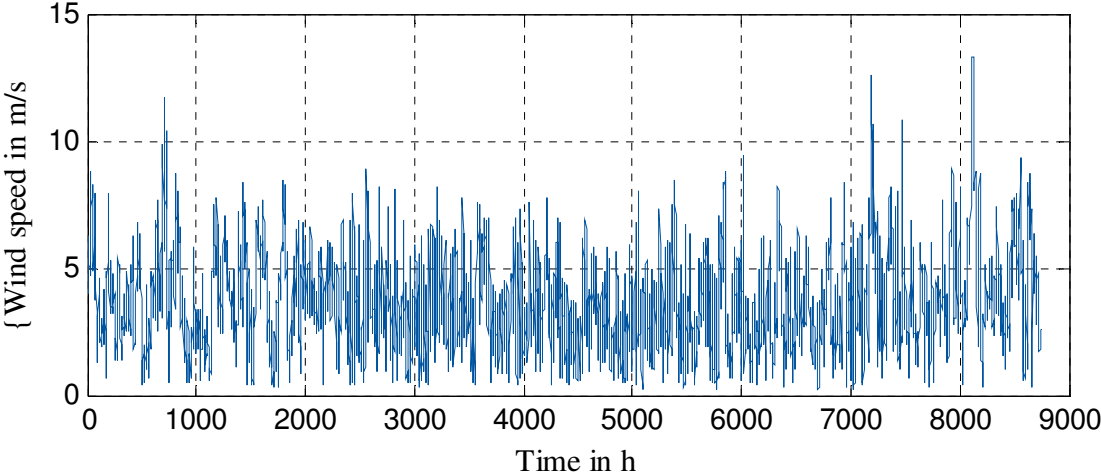
Figure 13 1-year wind profile of the location Feldberg
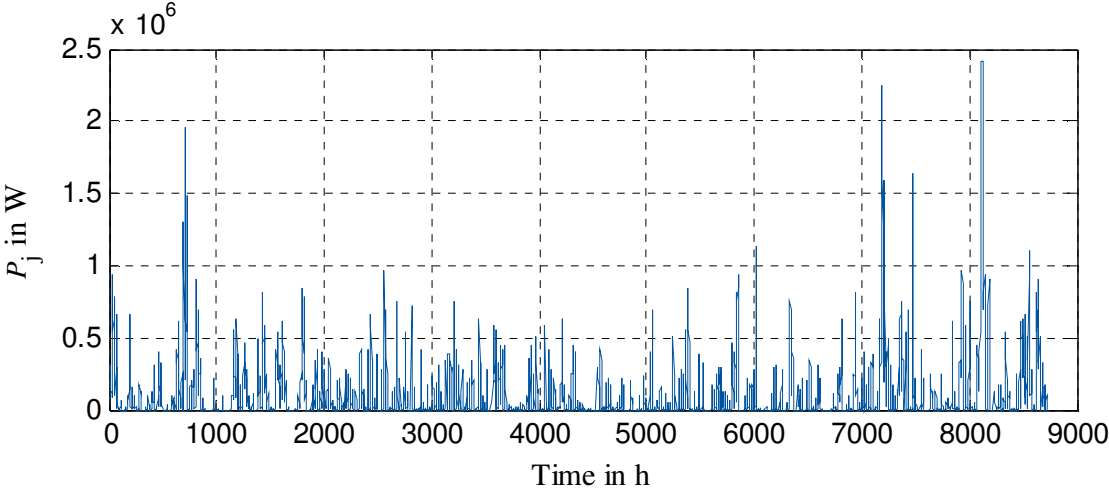
Figure 14 The resulting power profile of the wind turbine if installed in Feldberg
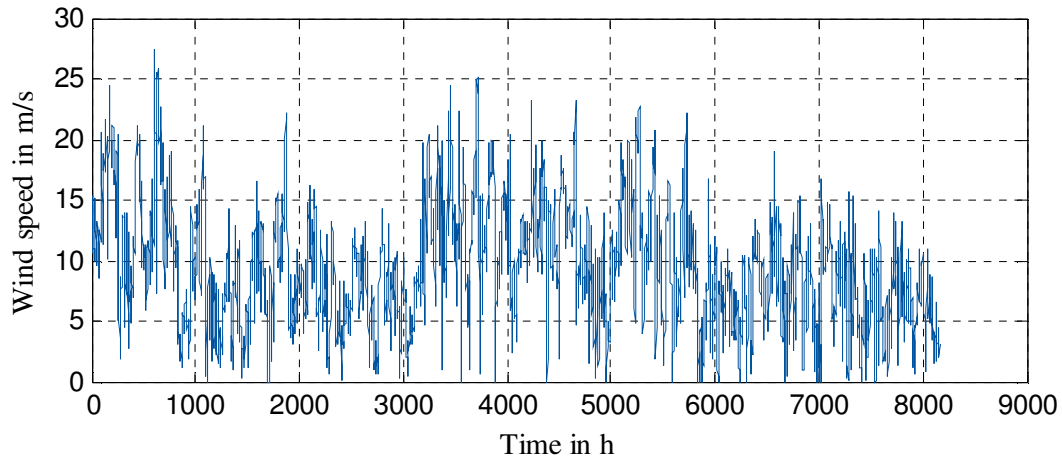
Figure 15 1-year wind profile of the location Niedersachsen
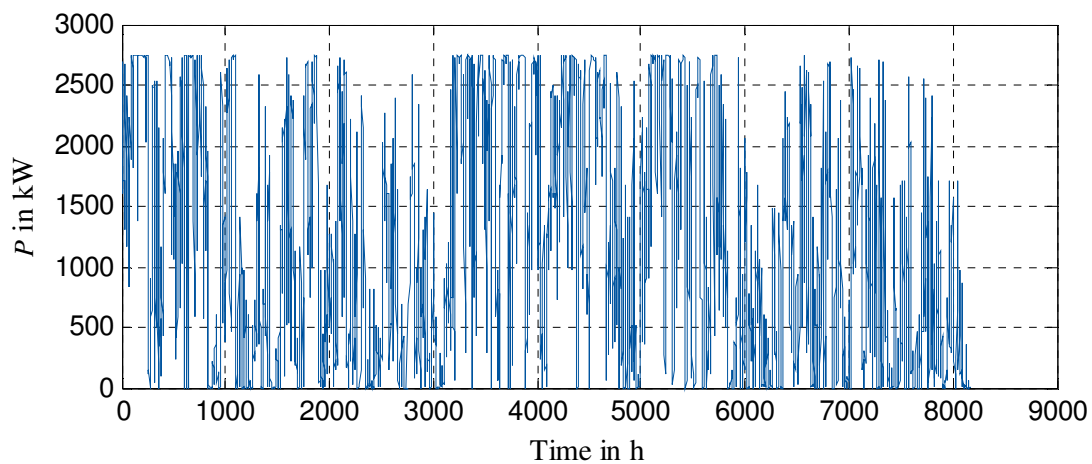
Figure 16 The resulting power profile of the wind turbine if installed in Niedersachsen

In order to retrieve the 1-year power profile, the following steps are followed. As an example, the wind profile of the location Niedersachsen depicted in Figure 15 and the power characteristic curve versus wind speed of the wind turbine in Figure 2 are taken. For every time step of the wind profile in Figure 15, Matlab registers the value of the wind speed. Then it finds this value in Figure 2 to likewise find the corresponding value of power to be placed in the new graph, the 1-year power profile Figure 16.

Matlab does the same procedure when plotting the temperature profile, but it uses the 1-year power profile instead of the 1-year wind profile. For example, Figure 16 instead of 15, and a Tj vs. Power graph instead of the wind Vs. Power graph; Figure 10, 11 or 12 instead of Figure 2. Afterwards, Figure 18 is obtained.

This procedure is used to obtain the 1-year arrays of Power and T_{j}.

The 1-year temperature profiles are the following: (For the sake of simplicity and quality with regard to information against dull abundancy, we selected the second design, at 40 ℃ of cooling temperature in both locations). As we can see on the following Figures, the work load of the IGBT's in the first location (Figure 17) is trivial in comparison to the ones in the second location (Figure 18), as the power generated is greater, the larger the power losses will be and more increments of T_j occur. This will have a noticeable impact once we realize the Rainflow algorithm.
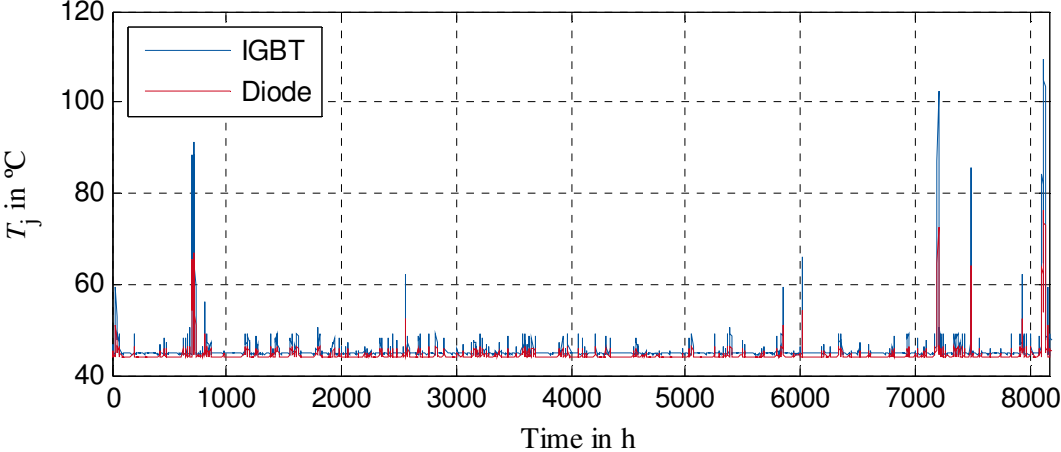
Figure 17 The resulting junction temperature T_j profile in Feldberg
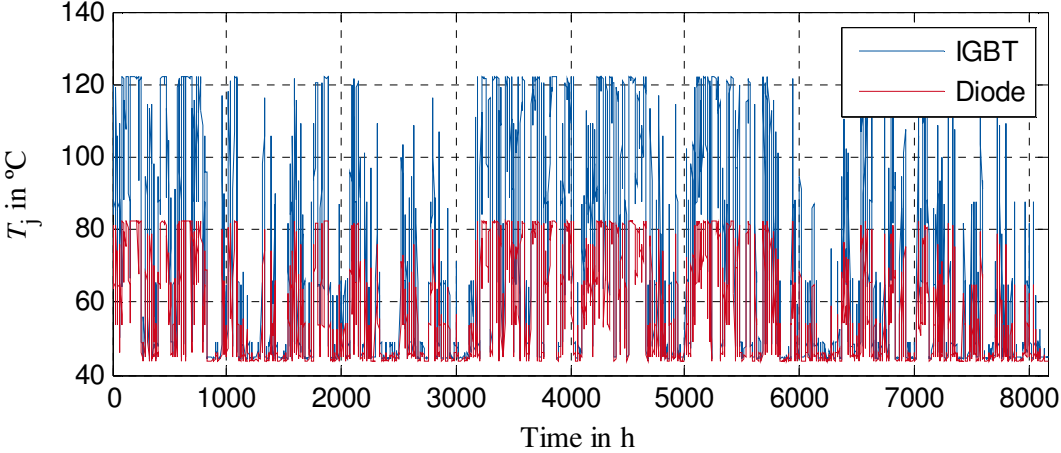
Figure 18 The resulting junction temperature T_j profile in Niedersachsen

4.2 Medium Term

The second model for the medium-term estimation represents the three dimensional wind field of the hardware in the loop from the center for Wind Power Drives. As inputs, a

turbulence of 18 % is fixed, which is the maximum turbulence intensity for wind turbines according to IEC 61400-1. The 18% is measured at the wind speed when it equals 16 m/s. The wind turbine itself is designed for 16% turbulence intensity. 18% is taken as the worst case scenario.

The wind turbine itself is classified as class IIb wind turbine according to IEC 61400-1 with annual average wind speed of 8.26 m/s and 16% turbulence intensity. One value of the average wind speed is selected for every simulation we wish to execute. As an output, an array of junction temperatures registered along every time step is acquired, in our case, during 300 seconds. We reckon this cycle time of 300 s sufficient to observe the development of the T_j as a constant wind speed is applied to the model, varying randomly due to the turbulence. We selected time step smaller than 1 s for the 300 s simulation to allow the use of smaller time steps when applying the Rainflow algorithm to check if they showed more harmful increments than the normal steps on the figures of seconds, though it was proved that greater time steps were the right scope for such a perception.

For this second milestone, we conducted 13 simulations for every design, from a wind speed of 4 m/s to one of 16 m/s, where the power produced is almost maximum. With these 13 simulations we obtain as an output 13 arrays, each representing 300 s. Due to memory issues, it is not possible to simulate three hours, therefore, the 300 s period will be extrapolated.

From Figure 19 to Figure 24, the simulation results of the junction temperature profile of the semiconductor devices for different wind speeds of 4 m/s and 16 m/s is plotted. In this simulation the turbulence intensity is set to be equal to 18%. While the second and third designs hold similarities in terms of reahced T_j, the graphs for the first design, though it has shape similitudes, do not reach such high T_j values as the other designs.

We start at 4 m/s and stop at 16 m/s due to the fact that prior to 4m/s, the momentum generated on the turbine is not enough for the generator to start, and beyond 16 m/s, the wind turbine will provide nearly constant nominal power, as it can be seen in Figure 2, so for 17 m/s to 25 m/s we can use the same array of data..
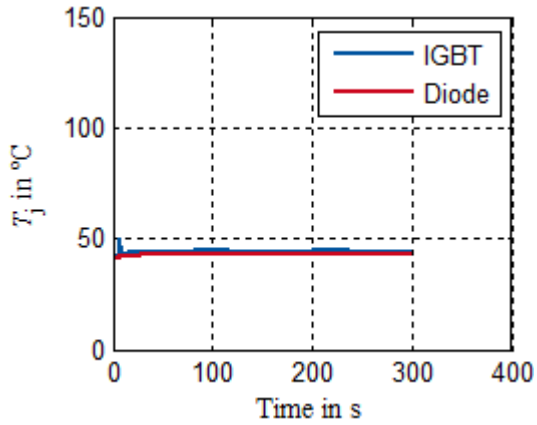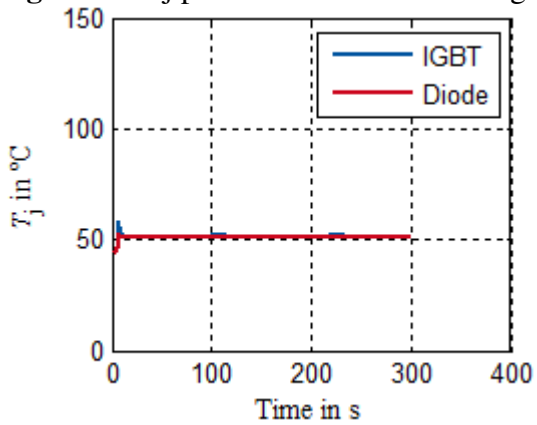
Figure 19 Tj profile for 4 m/s 1st Design
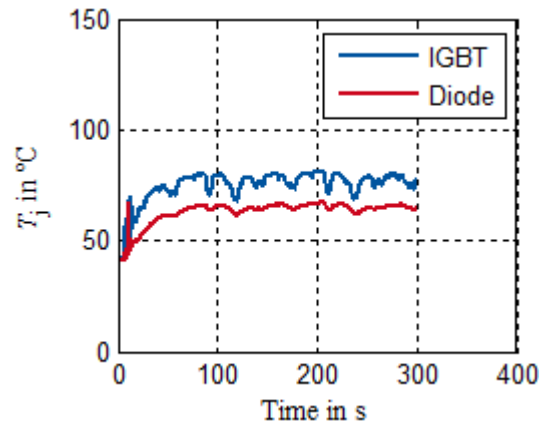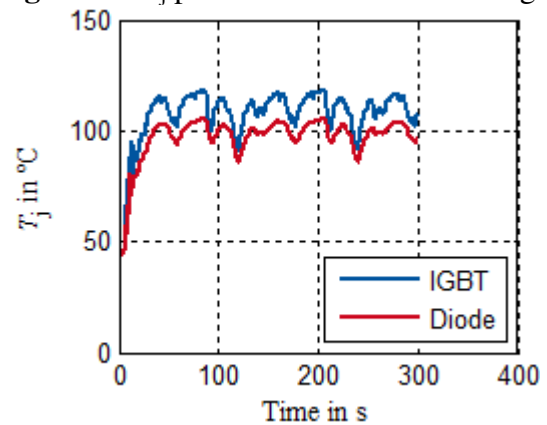

Figure 20 Tj profile for 16 m/s 1st Design
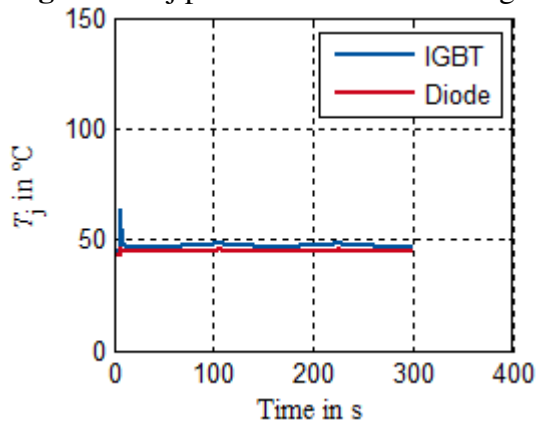
Figure 21 Tj profile for 4 m/s 2nd Design
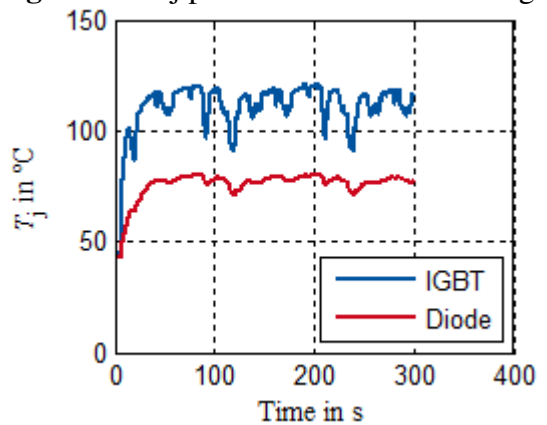
Figure 22 T_j profile for 16 m/s 2nd Design

Figure 23 Tj profile for 4 m/s 3rd Design


Figure 24 Tj profile for 16 m/s 3rd Design

5 Rainflow Algorithm & Lifetime Estimation

The Rainflow algorithm is used in the analysis of fatigue data in order to reduce a spectrum of varying stress into a set of simple stress reversals. Its importance is that it allows the application of different lifetime estimaton methods in order to assess the fatigue life of a structure subject to complex loading.

On the other hand, the lifetime estimation is a series of simple calculations that allow us to determine what its very name indicates. Even though the mathematical procedure is simple, in order to come to a result, there is the need of a tremendous data collection in order to fulfill the method. Datasheets are provided by the developers, their number of cycles until rupture is extracted from their own experimentation and extrapolations.

These lifetime-estimation methods are some times limited. As an example, the Coffin Manson expression in (2) cannot tolerate increments of temperatures smaller than 10 ºC which is often considered as the threshold at which the harmful effects occur, and the used cycle time is 2 seconds.

In the short-term estimation, 20 ms is the cycle time, so to even use the formula, extrapolation must be done beforehand. In the case of the medium-term, it might seem as the same conundrum going from 300 seconds to 3 hours. But we are extending the period to 3 h, for that is the period of study, and the method used is valid for 300 s and for 3 hours as well. In short-term, on the other hand, the formula is of questionable utility, as its constants numbers might not be sensible enough for the small changes in temperature we might have in a cycle time of 20 ms. Nonetheless, it can be used as a rough approximation in order to have an idea of how the real results might be.
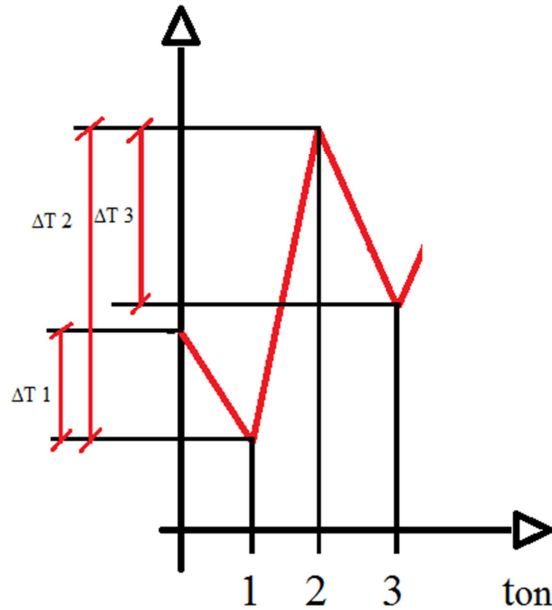
Figure 25 Rainflow algorithm process

Figure 25 represents how Matlab executes the Rainflow function. Points 1, 2, 3 are three sample points with a particular value of temperature assigned to each of them. The sample points from the temperature profiles coincide to the sample points Matlab's Rainflow algorithm would use. For instance, imagine our sample time was 1 hour, consequently, the sample time Matlab would use for the Rainflow (Also called t_{on}, as it is the time in which the ΔT is being studied and the stress is on going), would be of 1 hour as well.

The Rainflow algorithm will compare two consecutive points, for example, between 2 and 3. If it registers an increment lower than 10 ºC, it will continue comparing points 3 with 4. However, if it obtains a value greater than 10 ºC, it will calculate the T_{mean} of the increment and count one cycle at this T_{mean} with its ΔT, registering it in a file.

This t_{on}, sample time, corresponds with the time that the IGBT and diode endure the increment of temperature, which will be used in the lifetime estimation. For this, the data given by the developers from a graph of the datasheet needs to be extracted first. Figure 26 and Figure 27 are the two tables scanned.
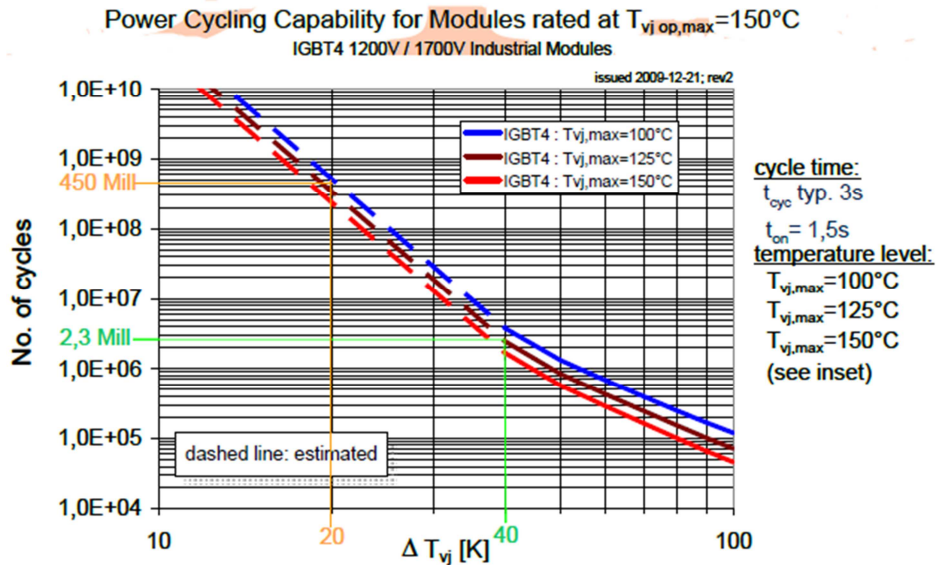
Figure 26 Number of cycles until rupture vs ΔT [8]

Figure 26 represents the number of cycles N$_{cycles}$ that the IGBTs can withstand until the rupture of the 10% of their population for every single increment of temperature ΔT. This is often called B$_{10}$ lifetime. The higher the increment of temperature is, the less N$_{cycles}$ they can endure. So for a 40ºC increment of 1.5 s (t_{on} of the developer's experiment), 2.3 million cycles of 3 s will occur until the 10 % of the population breaks down.
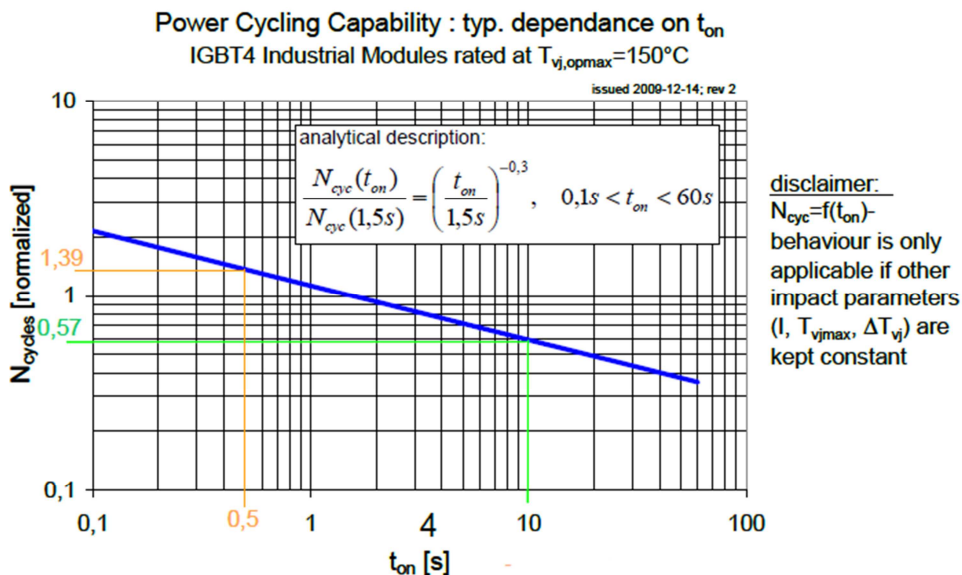
Figure 27 Coeficient to multiply number of cycles vs t_{on} [8]

Figure 27 presents instead, a coefficient that varies depending on the sampling time, t_{on}, which will be multiplied by the N$_{cycles}$ we obtain from Figure 26. The reason behind this step lies on

the fact that the effect of having an increment of temperature of, for example, 50 ºC during a t_{on} of 10 seconds is stronger than having it during 1.5 seconds, which is the t_{on} reference used in Figure 26. In the first case, the overall deformation will be larger than in the second case, as the dilation due to the 50ºC temperature would be longer, hence the necessity to compensate with this coeficient. Another matter to be attended before continuing is whether or not the fact of having the same cycle time (duration of the test) but different sample times will affect the end result.

T_{on} could be seen as a scope and the cycle time as the whole picture. We need to find the right t_{on} in order to register the details of the 1-year profile or of the 3 h profile (the whole picture) that will be the most harmful to the IGBTs, so as to acquire the most realistic data possible. All results are in part correct. However, depending on which t_{on} is used, we might see results that condone really important data. If t_{on} is small, we would have many small ΔT. If t_{on} is bigger, we will have not so many but greater ΔT. The question is which one will be more harmful to the power electronics devices. By simple calculations this question can be clarified, and with its conclussion, base the choosing of a sample time or another depending on what will show more deterioration on the IGBT's lifetime.

It can be put into consideration to use a variable sample time, t_{on}, depending on the increments we register, so as to take both on account, many small ΔT and big ΔT. It would be the best way of action, but if the importance in the shortening of the life-time of less number but greater ΔT is much larger than the one of many but smaller ΔT, then we can neglect partially the effect of these smaller ΔT and focus on the bigger ΔT with a bigger t_{on}, or viceversa.

We used data from Figure 26 and Figure 27 for an example:

The cycle time to be studied is of 10 seconds, this means that the object will be tested during this amount of time.

Firstly, we will use a sample time, t_{on}, of 10 seconds as well. This means that, according to Figure 26, the coefficient to multiply the Ncycles is $\left(\frac{10}{1.5}\right)^{-0.3} = 0.57$. Dividing 10 s of cycle time by 10 s of t_{on}, we obtain the Nº of samples taken. Let us say that this single measure registered is a $\Delta T = 40$ ºC. This increment corresponds to Ncycle = 2.3 million according to Figure 26, which needs to be multiplied by 0.57 because of the impact of a longer exposure than the reference of 1.5 s. The final result is of N_{cycles} =1.311 million cycles of 10 s until the 10% of the population is destroyed. This is equivalent to:

$$\frac{1.311 \times 10^6 \text{ cycles x 10 [s for every cycle]]}}{3600 \text{ [s in 1 hour]}} = 3641.67 \text{ hours} \tag{3}$$
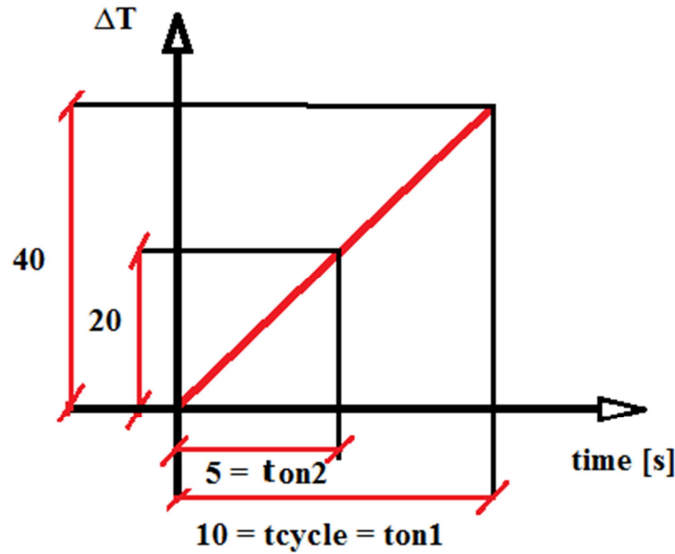
Figure 28 Explanatory diagram for the t_{on}

Figure 28 represents an explanatory diagram for t_{on}. Secondly, we use a sample time of 5 seconds, the coefficient from Figure 27 would equal $\left(\frac{5}{1.5}\right)^{-0.3} = 0.697$. In 5 seconds, we obtain 2 samples, meaning two $\Delta T = 20$ ºC. For this ΔT, the number of cycles is 450 million according to Figure 26. To bring them to scale to be compared, we need first to multiply it by 0.697, obtaining Ncycle= 313.58 million cycles of 5 s. To scale the figure again to the cycle time of 10 s, we obtain 313.58/2= 156.79 million cycles of 10 s until 10% of the population is destroyed:

$$\frac{156.79 \times 10^6 \text{ cycles x 10 [s for every cycle]]}}{3600 \text{ [s in 1 hour]}} = 435527 \text{ hours} \tag{4}$$

By choosing the second process, the user would be led to think that until $B_{10,}$ 119.6 times more hours would occur.

Concluding from this example, it is clear the necessity to give more importance to the greater ΔT. Other calculations should be done to make sure that this is true, but only by dividing by half the t_{on}, we are obtaining tremendous differences; which it is attributed to the fact that the distribution of the N_{cycles} is logarithmic, therefore there is no need for further calculations.

It was said before that the sample time used by Matlab cannot be changed, as it uses the same one used by our temperature profile, therefore this demonstration would be useless as a proper

t_{on} will not be able to be found. Even though that is true, there is a way to change this sample time if we simply crop the 1-year or the 3-h temperature profile. If we eliminate, for example, 3 sample points in between another 2, we have jumped 4 hours in time. So albeit the year array or the 3-hour array have been compressed, it still represents a year and we would obtain the same result as if we would have augmented the sample time of Matlab from 1 to 4 hours, as it only registers the value on the sample points.

With this been said, from Figure 26 we extract the 2 arrays (N_{cycles} and ΔT) corresponding to one of the drawn functions, these two arrays would be compared to the ones obtained from the Rainflow algorithm.

For the long term-estimation, the chosen function was the one with T_{j_max} = 125 ºC from Figure 26 for the second design and T_{j_max} = 80 ºC for the first design. To come to that decision, the maximum temperatures reached by each design were observed, being them 122.1ºC for the seconds design and the lowest 81.5 ºC for the first one, when producing the desired nominal power. We were able to obtain the 80ºC curve through interpolation and extrapolation process which will be explained in the following point.

All this applies to the first and second design. For the third one, as it comes form another manufacturer, we use the lifetime characteristic curve in Figure 29 and Figure 30.
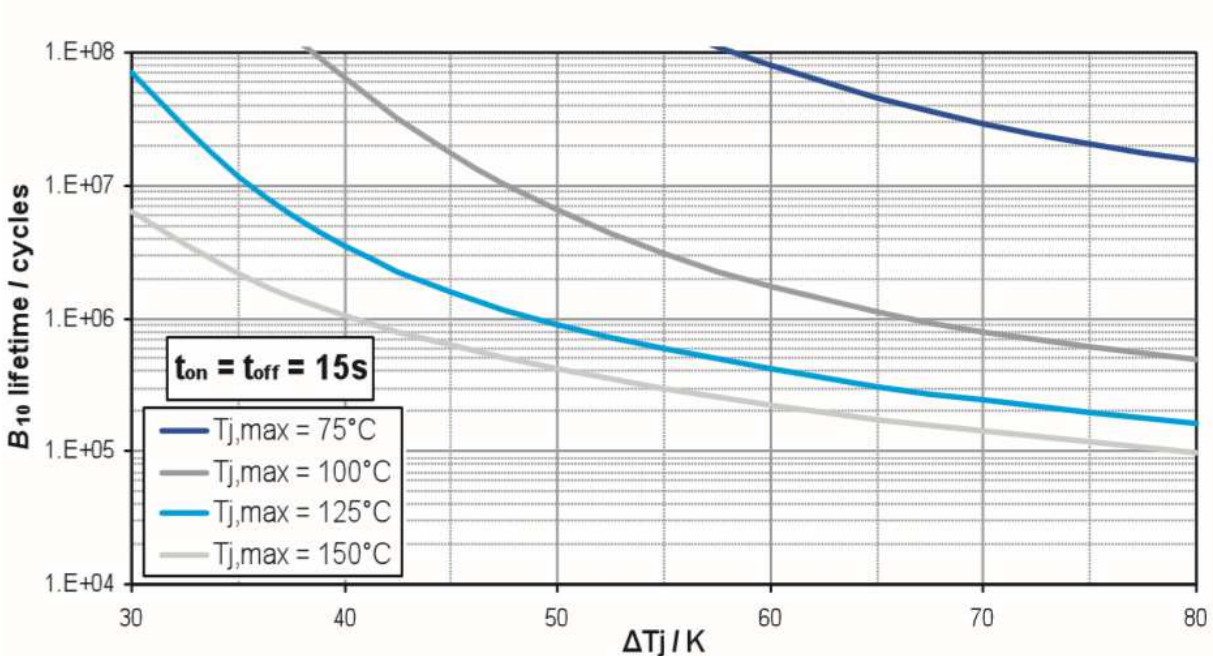
Figure 29 Ncycles Vs ΔT for a ton of 5 s
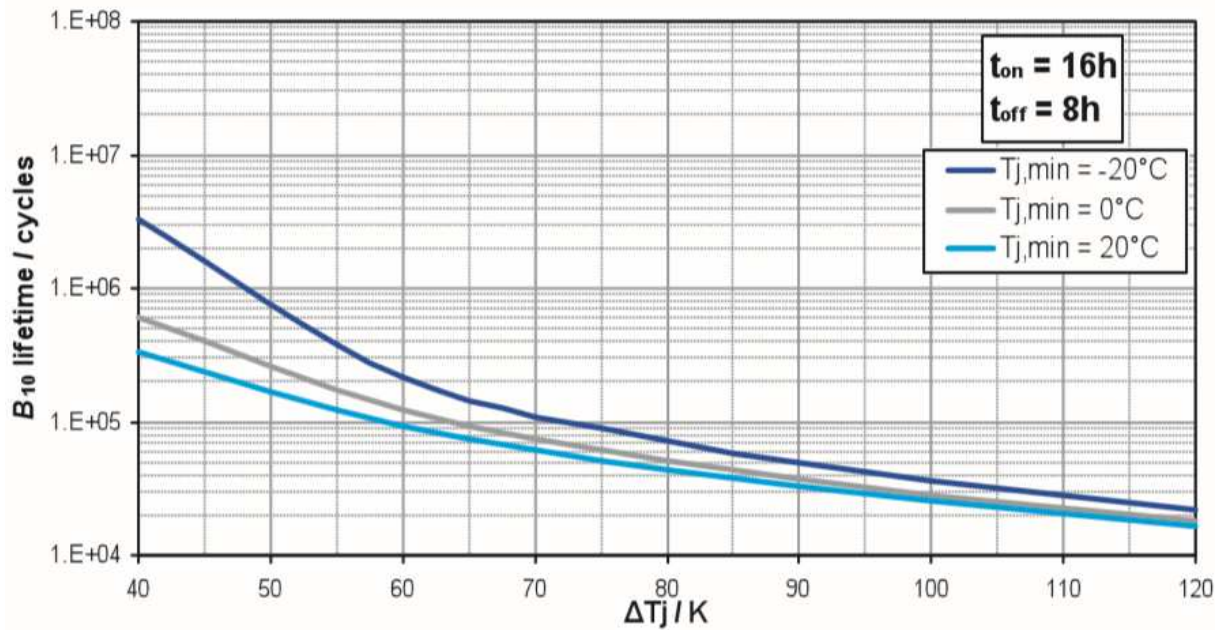
Figure 30 Ncycles Vs ΔT *for a ton of 16 h*

We will follow the same procedure as before, but as 15 s sample time for the medium-term estimation and 16 h sample time for the long term estimation are used for the third design, coinciding with the t_{on} of the graphs, no coeficients will be needed to be applied.

In Figure 30, we can see that the functions are T_{j_min}, therefore, for our third design, we will use 40 ºC, and as this 40ºC curve is not on the Figure 30 given, this function will be obtained thorugh extrapolation and interpolation.

5.1 Long-term

As it is the IGBT the device which reaches the highest temperatures and as the aim of this thesis is the study of the IGBTs, we will not consider the Diodes or the case for the life-time estimation. Although a study of the Diodes should be of interest as well in case of rectifier operation such as the machine-side converter.

5.1.1 Rainflow Algorithm

Once we obtain the one-year temperature profile of the IGBT, it is time to use the Rainflow tool. As a summary of what has been previously said, what this procedure accomplishes is to classify the different increments of temperature it finds along the provided 1-year temperature

profile. These increments were limited to be no less than 10 ºC, due to the reason previously explained and for the fact that such low increments of temperature do not affect drastically the lifetime of the IGBTs [4].

The Matlab Rainflow algorithm creates a 3 dimensional matrix, which classifies the ΔT depending on its T_{mean} and on the number of cycles (N_{cycles}), that the object has undergone. It also creates another 2 dimensional matrix, which does not take into account the T_{mean} to which every N_{cycles} and ΔT is assigned. As an example of the data, we will use again the toughest of conditons, the second location at 40ºC of ambient temperature of the three designs so as to see the difference between them.

The results from the Rainflow for the different designs are presented from Figure 32 to Figure 39. (T_A = ambient temperature)
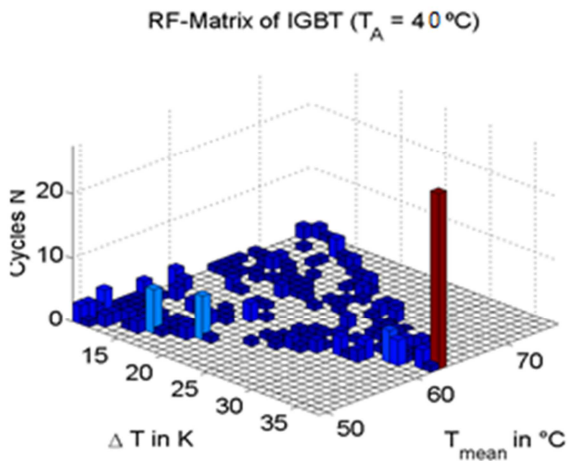
Figure 31 3D Results 1st Design 40 ºC Niedersachsen
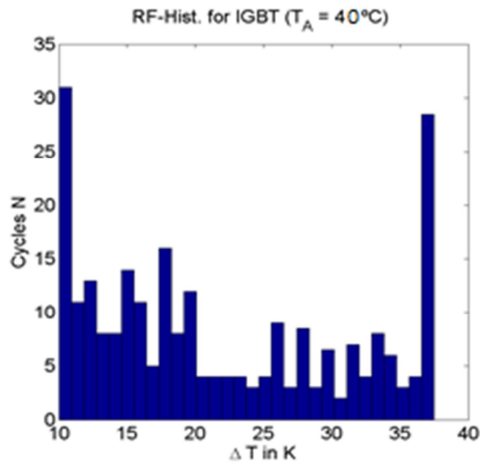
Figure 32 2D Results 1st Design 40 ºC Niedersachsen

RF-Matrix of IGBT (T_A = 40 °C)

RF-Hist. for IGBT (T_A = 40 °C)
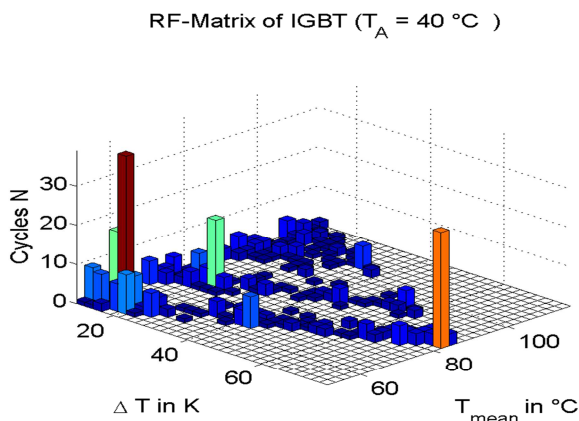
Figure 33 2D Results 2nd Design 40 °C
Niedersachsen
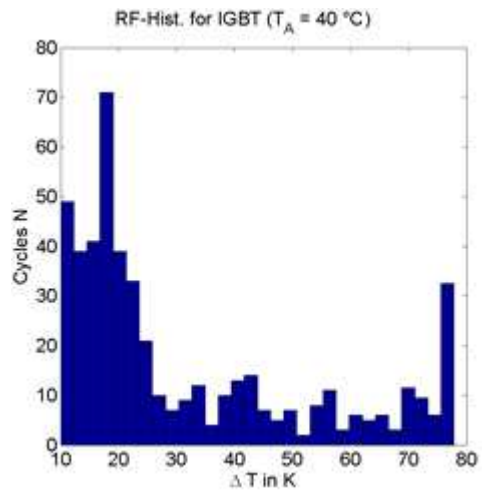
Figure 34 2D Results 2nd Design 40 °C
Niedersachsen

RF-Matrix of IGBT (T_A = 40 °C)

RF-Hist. for IGBT (T_A = 40 °C)
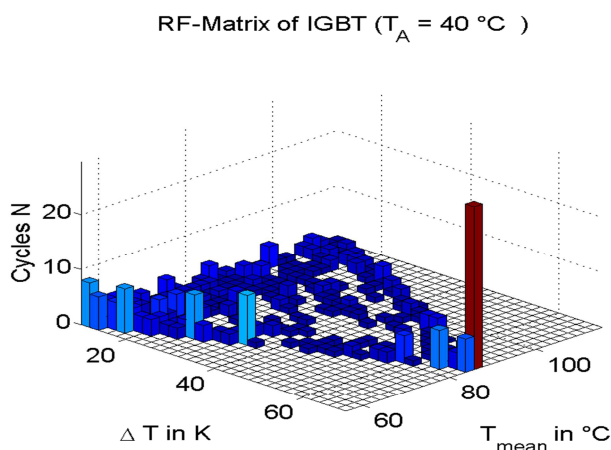
Figure 35 3D Results 3rd Design 40 °C
Niedersachsen
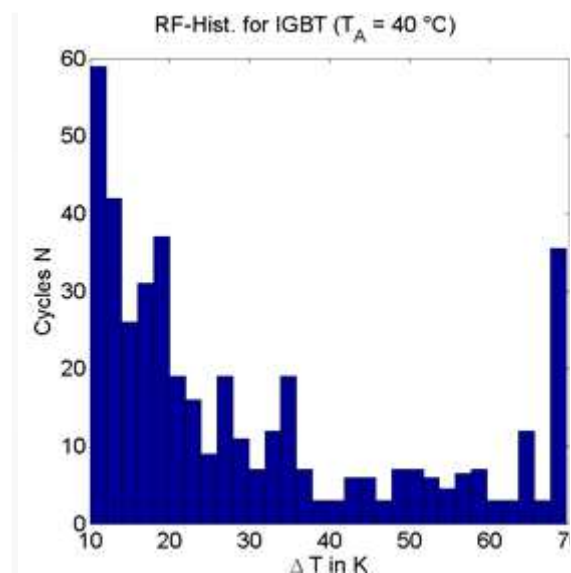
Figure 36 2D Results 3rd Design 40 °C
Niedersachsen

The number of cycles registered in the 2nd design is much greater than the ones in the 1st design, though more similar to the ones in the 3rd design, this will have repercussions in the final results as it will be shown.

In Figure 37 and 38, we can appreciate the contrary, the first design at the lowest wind intensity location at 40°C of initial temperature. With this we show once more how over-rated

this first design is and how the conditions of the first location are so mild they barely stress the components.
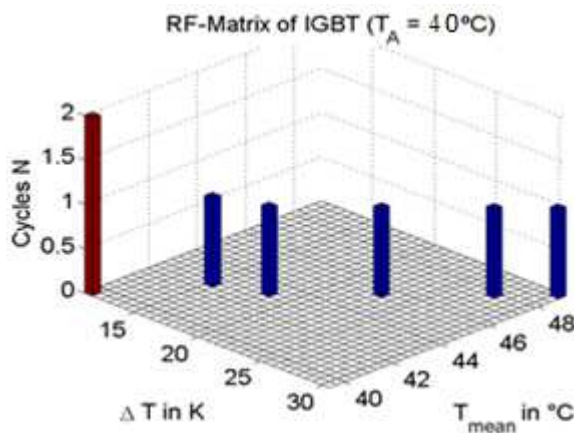
Figure 37 3D Results 1st Design 40ºC Feldberg
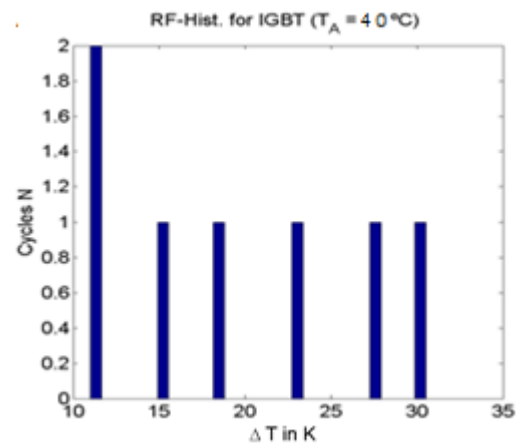
Figure 38 2D Results 1st Design 40 ºC Niedersachsen

As clarified before, we clearly can see the lack of cycles, therefore the stress that the over-rated model in mild conditions of wind intensity suffers.

5.1.2 Lifetime Estimation

Our work was to connect this raw data from the Rainflow algorithm with the given especifications from the developers and to come to a result. A complete new script was dedicated to this issue, following this algorithm:

To make it clearer along the explanation, we will name the arrays of ΔT and of N_{cycles} obtained from Figure 26 of the Manufacturer: ΔT_M and $N_{cycles, M}$; and the arrays from our Rainflow: ΔT_R and $N_{cycles,R}$.

- $N_{cycles,R}$ = Number of cycles at a certain ΔT endure by the IGBT per year
- $N_{cycles,M}$ = Number of cycles at a certain ΔT that the IGBT withstands until rupture

After, the matrix N_{cycles} from the Rainflow algorithm is compressed into one line array, $N_{cycles,R}$, as there are several N_{cycles} per ΔT and per T_{mean}. To be more visual, for example, it would be as if converting Figure 33 into Figure 34. This is done since the stressed caused by dilatation and contraction is due to the ΔT, its mean value does not take part on the deformation

$$N_{cycles,R}(\Delta T_p) = \sum_{k=1}^{n} N_{cycles,R}(T_{mean,p,k}) \tag{5}$$

Once that is done, through a loop, we compare the ΔT_R with ΔT_D, to select the N_{cycles} to be used from $N_{cycles,M}$. These will be the denominator of their corresponding N_{cycles} from $N_{cycles,R}$. We chose as sample time of 1 hour as we are studying one year, other t_{on} were also tried obtaining different results as it will be appreciated in point 6 where they are explained. Due to the fact that with one hour we obtain the most harmful results for the IGBT, we use 1 hour as sample time from the 1-year profile. The factor from Figure 27 which corresponds to 1 h is:

$$\text{Factor} = \left(\frac{t_{on}}{t_{on,ref}}\right)^{-0.3} = \left(\frac{3600 \text{ s}}{1.5 \text{ s}}\right)^{-0.3} = 0,968 \tag{6}$$

Finally we use the following formula:

$$N_{cycles,B10} = \frac{1}{\frac{1}{\text{Factor}} \sum_{k=1}^{n} \frac{N_{cycles,R,k}}{N_{cycles,M,k}}} \tag{7}$$

Thus, we obtain the number of cycles that the electronic devices will endure. Each cycle corresponds to a whole year, as that is our cycle time: $N_{cycles,B10}$ = Number of years until rupture of the 10 % of the population.

Therefore, in 20 years, the life-time consumed will follow Eq. 8 (Results shown in point 6):

$$\text{Lifetime consumed in 20 years} = \frac{20 \text{ years}}{N_{cycles,B10}} \times 100\% \tag{8}$$

5.2 Medium-term
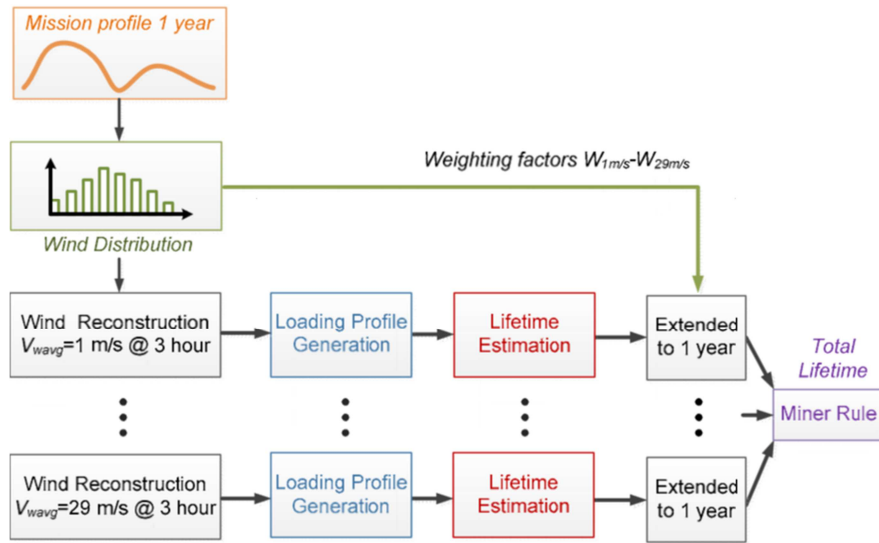
Figure 39 Block diagram of the medium-term lifetime estimation

For the medium-term lifetime estimation, once the 300 s temperature profiles for each studied wind speed are obtained, the sequence as depicted in Figure 39 is followed.

It is not as straightforward as in the long-term estimation. For each simulated wind profile, one temperature profile of 300 s is obtained, which is then extended to a 3-hour profile to follow a similar struture as other research papers [4] so as to normilise our work.

Each profile will be put through the Rainflow algorithm and to the lifetime estimation process which will be extended to one year afterwards, as it will later be seen. Once we obtain the life-time of the IGBT for each T_j profile, we apply Miner's Rule which consists of a summatory with a multiplication of every component by a coefficient based on the frecuency distribution of each average wind speed along the year, Equation 9. For example, the amount of time that the wind had a speed of 25 m/s might be lower than at 8 m/s, therefore the weight of the life-estimation coeficient for 25 m/s will be less than the one 8 m/s possesses.

5.2.1 Rainflow

This step holds the same principle as in the long-term estimation process. In that one, we interpolated the temperature to a 1-year profile and then applied on it the Rainflow algorithm. In this case, we obtain directly a 300 s profile of the Tj of the power electronics devices. To follow our esqueme, we extrapolate this data to 3 hours by means of a script which repeats the profile of 300 s, 36 times. Once this profile is obtained, we apply the Rainflow algorithm.

The script created will process these steps automatically for each profile obtained, from 4 m/s to 16 m/s, extracting 13 rainflow *structs* of data containing for each wind speed: ΔT, T_{mean} and N_{cycles}. (The reason why we use only these profiles is explained in point 4.2).

5.2.2 Lifetime Estimation

For this lifetime estimation, we adopt a sample time of 15 s. It was also taken into account that as we use every different temperature profile, we would also need to vary the function selected from Figure 29 as the maximum temperature will progressively change. Owing to this, for this medium-term stimation, a new graph was created from Figure 29 to obtain the proper functions, Figure 41, for each maximum temperature that the temperature profiles might hold. It can also be said the same about Figure 26, obatinig Figure 40.

To create Figure 41 from three previous functions in Figure 29, exponential extrapolation was used between the points, as it is this interpolation method the one that best describes the physics involved in this case. Cubic interpolation, on the other hand, often gives undesirable inflexion points, but exponential interpolaton allows avoiding these inflexion points and contains cubic splines as special case [6].
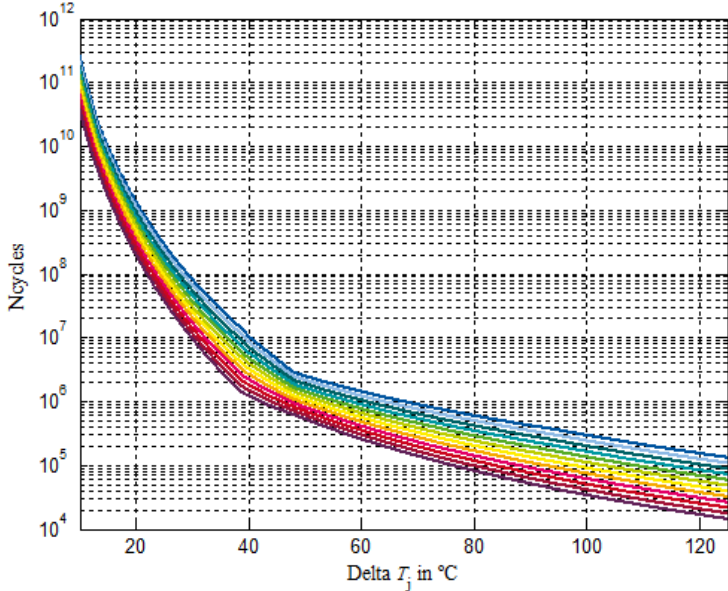
Figure 40 Espectrum of curves for each Tj_max 1st and 2nd Design
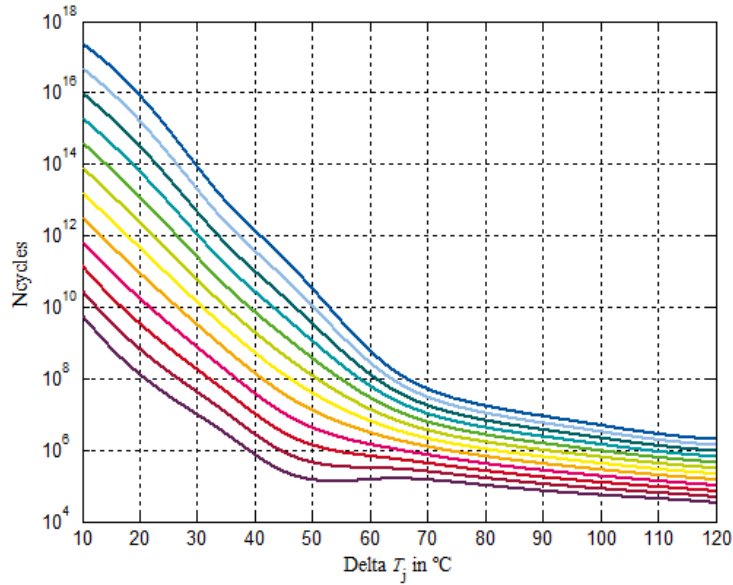
Figure 41 Spectrum of curves for each Tj_max 3rd Design

Then again, this step holds the same principle as in the long-term estimation (Eq. 5, Eq. 6 and Eq. 7 are also used for each wind profile Rainflow data).

Once the 21 lifetime cycles are obtained for the 21 avarage speeds, from 4 m/s to 25 m/s, Minor's rule is applied and extended to one year, as it follows in Eq. 9, obtaining the lifetime consumed in 1 year.

$$\text{Lifetime} = \frac{\text{Number of total cycles per year}}{\text{Number of total possible cycles}} = \frac{365 \text{ year} * 24 \text{ hours}}{3 \text{ hours}} \times \sum_{k=1}^{25} \frac{W_k}{N_{cycles,B10,k}} \qquad (9)$$

A matter of interest is the weight coeficients W_k. In the long-term lifetime estimation, the 1-year wind profile affects indirectly to the lifetime, since the kind of T_j profile depends on it. In this medium-term lifetime estimation, the 1-year wind profile affetcs directly on the coeficients. We follow two methods:

The first, as we are studying two locations, Feldberg and a location in Niedersachsen, from the measured wind profile over one year, the distribution coefficient of every wind speed can be extracted. For each wind speed, we obtained a percentage of the time along the year the wind speed had been present, and that percentage will be multiplied to the corresponding number of cycles in one year. For example, according to the data, we obtain the following distribution curves in Figure 42.
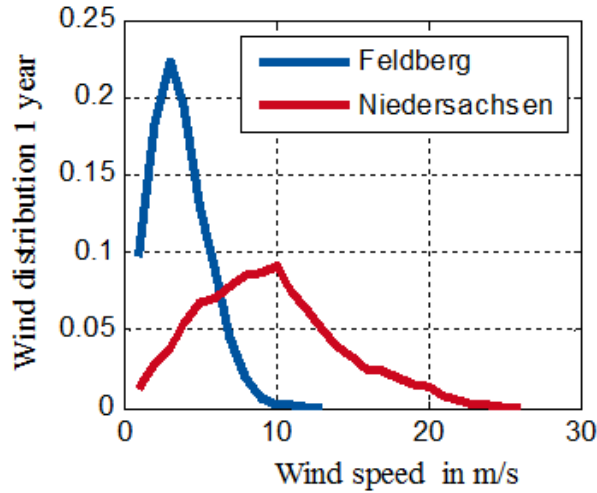
Figure 42 Probability density distribution of wind speeds in Niedersachsen and Feldberg

We can appreciate again the lack of wind intensity in Feldberg, as the maximum wind speed is around 13 m/s and barely had appeared in the year as the low percentage shows. With this coeficients we obtained accurate medium-term life-estimation results, as we used the raw data from the weather stations. Although this would not be so interesting, if a general idea of the lifetime behaviours of the power electronics devices is sought.

Due to this, we also used a second method to obtain the weights to calculate a larger range of data and see how the distribution of the wind speed along the year affects the life-time of the devices. For this second approach we used a Weibull distribution, Eq. 10, as it describes almost perfectly the distribution of the wind speeds in one year.

$$f(x; \lambda, k) = \begin{cases} \frac{k}{\lambda} \left(\frac{x}{\lambda}\right)^{k-1} e^{-\left(\frac{x}{\lambda}\right)^k}, & x \geq 0 \\ 0, & x < 0 \end{cases} \qquad (10)$$

This is simply the distribution of the proportion of time spent by the wind within narrow bands of wind speed. In our case: 4, 5, 6… 25 m/s.

We select the shape paramenter k, as constant and we will vary the scale paramenter λ, from 6 to 10 to get various dsitributions to sample the extremes and set the behavior on the limits. This λ interval is the one that lies within the normal range of real wind distributions. Therefore, if we obtain the wind distribution of another location, there is no need to simulate once again with the new data, only check the look-up table for the value of λ closest to the one given from this location. On Figure 43 can be seen the effects of varying the value of λ.
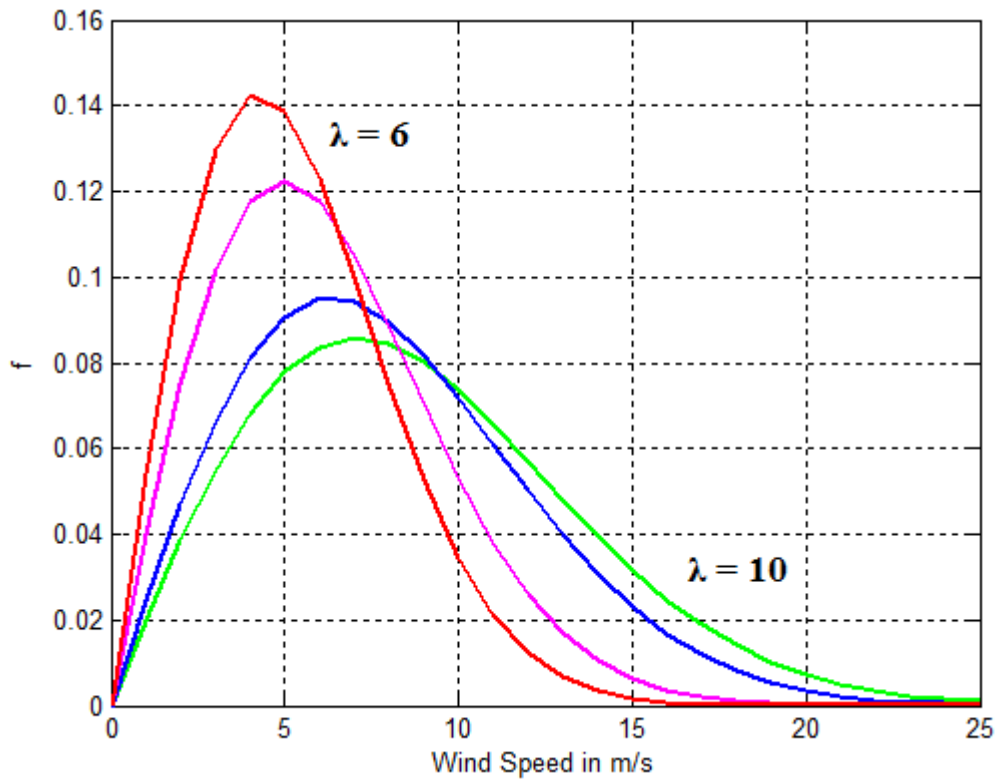
Figure 43 Weibull distribution for different scale parameters

6 Results

6.1 Long-term

Table 6 represents the first design as a value reference. This is done to observe whether this oversizing is worth it or not. It is clearly seen, that by placing in parallel one more module for each previous one, the lifetime B_{10} of the IGBT's increasses 88.48 times in Feldberg and 70.34 times in Niedersachen, values which are around the same order. Therefore, this oversizing is of interest and should be taken in consideration before designing power electronics converters. Design 3 cannot be included as it belongs to another manufacturer.

Table 6 Long-term estimated lifetime normalized to the original design (T_{water} = 40ºC)

	Feldberg	**Niedersachsen**
1st Design (Reference)	1	1
2nd Design	88.48	70.34

The results for the first experiment on the IGBT's are represented in Table 7 individually and in percentage, for 40 ºC of ambient temperature with 1 hour sample time in a 20 years spectrum, B_{10}:

Table 7 Results of the estimated lifetime (T_{water} = 40ºC)

	Feldberg	**Niedersachsen**
1st Design	0.00117542 %	0.134 %
2nd Design	0.104 %	9.426 %
3rd Design	1.078 %	35.812 %

So as to have an idea of what these values represent, let us take 9.426 % from the second design. With regard to what was previously explained, this percentage means that a 10th of the population will have consumed in 20 years the 9.426% of the total $N_{cycles,B10}$ they can endure until rupture, or what is the same, they have consumed 9.426% of their time until rupture. This implies likewise that this tenth of the population will consume their entire life time in aproximately 212 years.

Looking at the other data, the life-time of the first design is barely affected, indicating that a 10th of the population would last an enormous amount of time. The same can be said about the experiments with Feldberg as location, they do not reach high values whatsoever if compared to the ones in Niedersachsen. Though this might seem deterministic, this study only refutes the possibility of failing due to the causes taken on account in this paper, which were derived from the manufacturers. Therefore, by no means it could be understood as if they could last for such a period of time, other problems not studied in this paper might occur causing their break down.

The values for the third design from the second manufacturer could be taken aback when seeing that they are greater than the ones from the second design, even though the Rainflow showed similar $N_{cycles,R}$ in both. While this is true, the properties for each IGBT are different as it can clearly be seen between Figure 26 and Figure 30. The third design is much weaker with regard to the number of cycles which can withstand.

But this direct relationship between the results from the Rainflow algorithm and the life-time estimation can, on the other hand, be correctly distinguished if comparing the first and second benchamark as both belong to the same manufacturer. The first design undergoes clearly, seeing Figure 31 and Figure 32, less amount of stress cycles than the second design, Figure 33 and Figure 34. This difference in stress is represented by an augment of well above a 100 % on the lifetime estimation results, e.g, from 0.134 %, 1st design, to 9.426 %, 2nd design.

The same can be said comparing the two locations, e.g 2nd design, 0.00117542 % in Feldberg against 9.426 % on Niedersachsen. It is clearly seen, looking at the Figures mentioned previously, that the number of cycles in higher increments of temperatures has indeed a greater effect on the life-time final results, even though they overall do not look threatening.

The question of whether or not the sample time plays an important rolle in this estimation has also been answered. Different sample times have been used in the Rainflow to check its further repercussion in the lifetime estimation.

We went no further than above a day of sample time, as even though the developer's datasheet has a function which theoretically holds any sample time, the graph given only goes up to 1 min, as we can see in Figure 27. Therefore even 24 hours might be too big of an extrapolation for the data given, but then again, that was the only table that the manufacturers provide. It would also not make sense to choose a sample time of one minute, within the scale, because we are focused on the long-term effects, meaning changes in the size of hours.

Here is Figure 44, which shows the different lifetime results for the different sample times for the 2nd design in Niedersachsen. (Only with 1,2,3,4,5,10, 16 and 24 hours sample time were tested, the decrease from 10 to 24 shall not be so drastic)
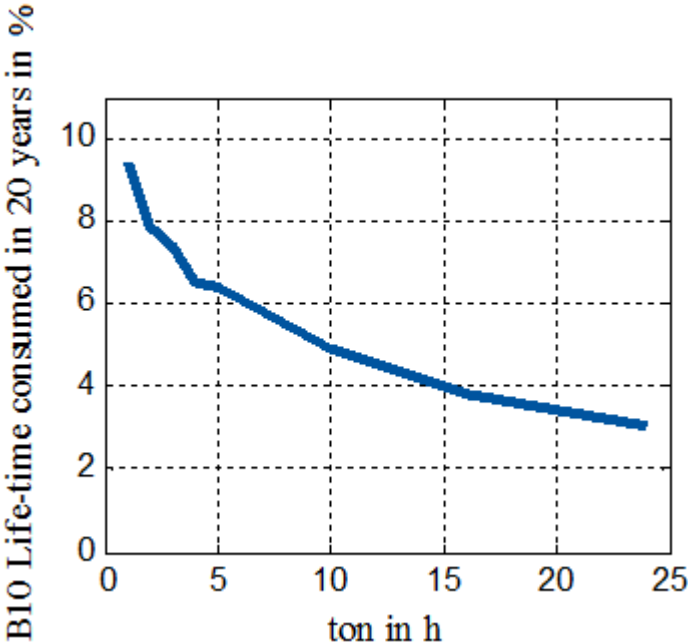
Figure 44 Sample time in h vs estimated lifetime

As it can be appreciated, there is a noticeable difference as we augment the sample time. The biggest loss of lifetime is obtained with a sample time of 1 hour, which means that 1 hour is the right scope for the Rainflow algorithm to find the most harmful data to the IGBT's. We also took 24 hour sample time to gather whether such big sample times are adequate or not. Looking at Figure 44 we can certainly say they are not adequate. There is room for more experimentation, but looking at the overall result, we can assume that greater sample time show less harm in the IGBTs.

6.2 Medium-term

The estimated B10 lifetime in 20 years for the second experiment on the IGBTs are represented in Table 8. The results are obtained with 40 ℃ of ambient temperature, 15 s of sample time.

Table 8 Resuls medium-term at a water cooling T of 40ºC

	Feldberg	**Niedersachsen**
1st Design	0.03 %	1.164 %
2nd Design	0.028 %	2.258 %
3rd Design	0.15 %	4.642 %

It can be seen that the over all results are much smaller than the ones obtained in the long-term estimation. Only in the 1st design the values are geater than in its previous experiment. That is interesting as it does not happen to the other 2 designs, therefore, we can reason that for over-rated devices, the medium-term effects play a greater roll than the long-term.

If indeed the 1st design is not over-priced, looking at the big differences between the 1st and the other two designs, it should be taken into account the possibility of introducing over-rated designs instead of optimal ones.

Aside from this fact, the wind of Feldberg represents again its lack of intensity when compared to Niedersachsen, increasing the values of the life-time estimation from one location to another by well above 100 % again, but they still seem not to have an alarming importance.
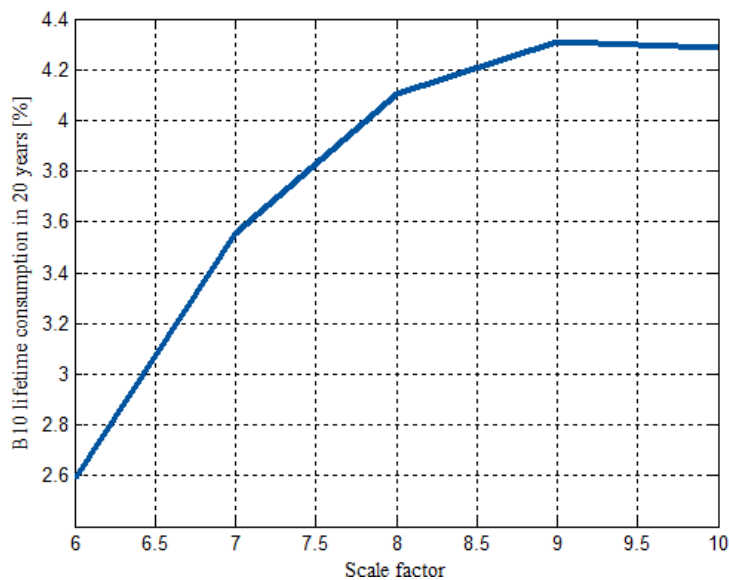
Figure 45 Resuls medium-term for a varying λ

We also studied, for the third design, the results of the life-time, B$_{10}$, depending on λ.

The greater the sacle factor, λ, is, the more spreaded the probability density formula will be. Hence, the lifetime will be reduced faster. It is interesting to note in Figure 45, whose data has been obtained from the 3rd design, that it is not at 10 but at a scale factor of 9 when the lifetime is the shortest (not by much), but it is something to take into account. Due to this spreading of higher λ, high wind speeds are more present along the year, which will consequently provoke the generation of the nominal power for longer, attaining larger power losses for the greater power generated. These greater power losses will increase the temperature, and the greater the power losses are, this increments will oscillate in greater size, provoking a shorter life span. This holds the same for the rest of the designs.

7 Conclussions and Outlook

7.1 Conclusions

It could be seen that the results from the long-term estimation could be condoned as they are really low. Therefore, the ones from the medium-term could also be seen as harmless and even negligible in comparison.

Looking at the over-rated design, only taking in consideration the assumptions gathered along this paper, it is not worth to invest in this over-sizing, as the other designs still hold low percentages of B_{10}. However, there is one matter to take into account, commented on point 7.2.

Overall, the life-time estimation results obtained in this paper might seem to be unimportant for the longevity of an IGBT, but they are not conclusive whatsoever. They represent the bases whence new research can further absolute conlussions.

7.2 Outlook

There are indeed various farther issues that could be considered to be revised.

A research over the importance of the short-term factors over the life-time of the IGBT's could be realized to complete the circle. This would not hold for the grid side inverter studied in this thesis, where the frequency is of 50 Hz. For the machine side rectifier, on the contrary, where the frecuency obtained from the generator is usually less than 40 Hz, where this phenomenom takes place, the study of the short-term lifetime estimation could be done.

Though in this paper it has been concluded that the long- term and medium-term estimation do not hold great imporatnce, the manufacturer tables whence we have extracted the N_{cycles} (Number of cycles, of a specific time length, until rupture of the IGBT) for our evaluation, do not consider if these curves would be maintained as such over the passing of the years. Meaning that for every year, the N_{cycles} extracted from the graph might gradually descend in value along time provoking a general faster decrease in their life time.

As an example, taking as if these N_{cycles} decrease every 20 years, saying that the 10th of the population of the 2nd design would last 212 years, would be incorrect, as not every 20 years 9.426 % would be consumed. If this calendric decrease in Ncycles would hold true, for the second period of 20 years, this percentage of 9.426 might rise due to the less amount of N_{cycles}

then allowed, doing so as well in the third period and so on. This is an example for every 20 years, but if such decrease in Ncycles exits, it might as well be treated per year, being then more drastic.

It could be noted as well, that the over-rated design (1st design) is practically not affected by these cycle stresses. If the N_{cycles} do not hold a calendric life-time, then the use of this over-rated IGBT would not be needed, as the other designs have also low percetages of B_{10}. But if the N_{cycles} is decreasing over time, it might be a good solution to invest in the first over-rated design in order to avoid the loss of IGBTs along the years.

Therefore, to definitively conclude whether or not these thermal cycles play a part in the life-time of the IGBT's, studying if these manufacturer's tables hold a calendric life-time could also be realized. And once this inquiry is fulfilled, seeing the much lower impact on the life-time the over-rated IGBT posseses and considering how much of a larger investment their purchase and installation would require, it could be pondered whether or not to consider this investment to overcome the possible malfunctions of the system, only in case the N_{cycles} from the manufacturers do hold a calendric life-time.

List of Figures

List of Tables

List of Equations

Bibliography

[1]   Neg Micon A/S, *Hauptspezifikation_NEG_Micon_NM80*. Denmark, 2013.

[2]   Neg Micon A/S, *Technical Description_NM80.* Denmark, 2003.

[3]   Infineon Technologies AG, *Infineon-AN2008_03: Thermal equivalent circuit models*. Warstein, 2008.

[4]   Ke Ma, Marco Liserre, Frede Blaabjerg, *Lifetime Estimation for the Power Semiconductors Considering Mission Profile in Wind Power Converter*. Aalborg, 2014.

[5]   Ke Ma, *Promising Topologies and Power Devices for Wind Power Converter*. Department of Energy Technology, Aalborg University, 2015.

[6]   H. Spfith, *Exponential Spline Interpolation*. Karlsruhe, 1968.

[7]   ABB Switzerland Ltd, *ABB HiPaK*. Lenzburg, Switzerland, 2013.

[8]   Ifineon Technologies AG, *Technical Information IGBT modules*, Warstein, 2010.

[9]   Plexim GmbH, User Manual Version 4.0, Zurich, Switzerland, 2016.

[10]   Power Electronics department, *Power Electronics technologies*, Zaragoza University, Spain, 2014.

[11]   Infineon Technologies AG, *techncal information FF1000R17IE4,* Warstein, 2014.

[12]   ABB Switzerland Ltd, *techncal information* 5SNA 1600N170100, Switzerland, 2013.